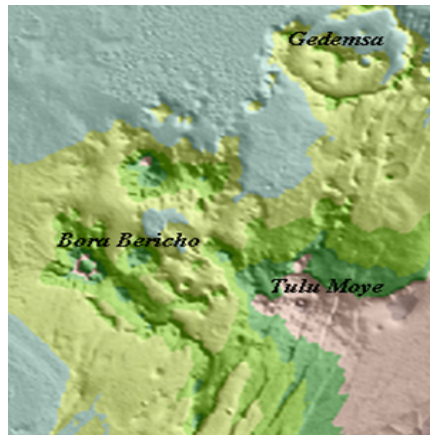




ADDIS ABABA UNIVERSITY
SCHOOL OF GRADUATE STUDIES
DEPARTMENT OF EARTH SCIENCES

**Structural Study and Its Effect on Thermal Activities of
Tulu Moye-Gedemsa Area**



A thesis Submitted to the School of Graduate Studies in partial fulfillment for the degree of masters of Science in ***Structural Geology- Tectonics and Rock Mechanics***

By: Engdawork Admassu Bahiru

July 2007
Addis Ababa



ADDIS ABABA UNIVERSITY
SCHOOL OF GRADUATE STUDIES

**Structural Study and Its Effect on Thermal
activities of
Tulu Moye- Gedemsa Area**

Thesis
Submitted to
The School of Graduate Studies of
Addis Ababa University

In partial fulfillment for the degree masters of Science in
Structural Geology-Tectonics and Rock Mechanics

Engdawork Admassu

July, 2007

ACKNOWLEDGMENT

I gratefully acknowledge my advisor; Dr. Bekele Abebe for his closeness and as he gave me not only valuable and constructive advises and comments but also provided me a good working environment for the progress and success of this study.

Special acknowledgment to Micheal Buchwitz, Thomas Heinig, prof. Richared Gloaguen and Khalid Adem all from Frieberg University of Germany for their vital advises and comments during the field work. They also provided me important articles, maps and photos, which are really helpful for the preparation of this work.

My thanks also goes to Dr. Birehanu Gizaw for his valuable advise at the beginning of the work especially on the geothermal part of the study.

It is my pleasure to acknowledge my friends from Geological Survey of Ethiopia for their help in guiding and giving me different GIS soft wares and written materials.

Immeasurable thanks goes to my beloved family, Admalem & Madublen, as they are always on side of me, wish my success and worry for my *well – being*.

Finally, local people of the study area are highly acknowledged for their vital information to reach at different sites of the area.

TABLE OF CONTENTS

<i>Contents</i>	<i>Page</i>
Abstract.....	I
Acknowledgment.....	III
List of Figures.....	VI
List of Tables.....	VII
List of Appendices.....	VII
List of Abbreviations.....	VIII
1. INTRODUCTION	1
1.1 Background.....	1
1.2 Geography.....	3
1.2.1 Location and Accessibility.....	3
1.2.2 Physiography and Drainage.....	5
1.2.3 Climate, Vegetation and Soil.....	7
1.2.4 Review of Previous Works.....	8
1.2.5 Objectives.....	9
1.2.6 Methods and Materials used.....	10
1.2.6.1 Methods.....	10
1.2.6.2 Materials used.....	11
2. GEOLOGY.....	12
2.1 Geology of Ethiopian Rift.....	12
2.1.1 General geology.....	12
2.1.1.1 Kella Basalt.....	14
2.1.1.2 Shebele Trachyte.....	14
2.1.1.3 Guraghe Basalt.....	14
2.1.1.4 Butajira Ignimbrite.....	14
2.1.1.5 Chilalo Trachyte.....	14
2.1.1.6 Wonji Group.....	14
2.1.2 Structural Framework of Main Ethiopian Rift (MER).....	15
2.2 Geology of the Study Area.....	18

2.2.1 Lithology.....	18
2.2.1.1 Pantelleritic ignimbrite and unwelded tuff	18
2.2.1.2 Basalts	19
2.2.1.3 Pyroclastic Cones.....	20
2.2.1.4 Obsidians, Trachytes and Lava domes.....	21
2.2.1.5 Alluvials deposits.....	21
2.2.2 Structural Interpretation of the Area.....	23
2.2.2.1 Fault Morphology	27
2.2.2.2 Formation and Growth of Faults in the study area	30
2.2.2.3 Fault Models	40
2.2.2.4 Fault Kinematics	42
3. FAULTING AND MAGMATISM.....	44
3.1 Cone – Fault interaction.....	48
3.2 Cone – Lava flow interaction.....	49
3.3 Fault – lava/ basaltic flow interactions.	50
4. GEOTHERMAL ACTIVITY.....	52
4.1 Application of remote sensing in geological investigation.....	58
4.2 Interpretation of Land Surface Temperature (LST).....	59
5. CONCLUSION AND RECOMMENDATIONS.....	62
6.1 Conclusions.....	62
6.2 Recommendations.....	63
REFERENCE:	64
APPENDICES:.....	71

ILLUSTRATIONS

1. List of Figures

Figure 1.1 Location Map of the study area.....	4
Figure 1.2 Study area from Landsat image.....	5
Figure 1.3 Topographic map of the study area from 3 DEM.....	6
Figure 2.1 Geological sketch map of the Main Ethiopian Rift.....	15
Figure 2.2 Lineament map across the MER.....	17
Figure 2.3 Relatively weathered ignimbrite.....	19
Figure 2.4 AA and pahoehoe type basalts.	20
Figure 2.5 Pyroclastic cone.....	20
Figure 2.6 Obsidian dome.....	21
Figure 2.7 Hanging wall covered by alluvial deposit.....	21
Figure 2.8 Geological map of the study area.	22
Figure 2.9 DEM of southern part of the study area.	25
Figure 2.10 Tectonic map of the study area.....	26
Figure 2.11 ASTER image.....	27
Figure 2.12 Fault morphology profiles.....	28
Figure 2.13 Fissure morphology profiles.....	28
Figure 2.14 Morphology of the fault along its length.....	29
Figure 2.15 Faults dying out at the cones.....	30
Figure 2.16 Normal faults showing a proportion between their length and their throw.....	32
Figure 2.17 An open normal fault with vertical wall.....	33
Figure 2.18 Relatively matured fault with out any opening..	34
Figure 2.19 A fault with tilted hanging wall and significant opening.....	34
Figure 2.20 Arrow showing deep open fissure in Deneba.....	35
Figure 2.21 Map with the three phases of faulting..	35
Figure 2.22 Field sketch map of a representative open normal fault.....	37
Figure 2.23 Termination of a fault, open fissure.....	38
Figure 2.24 Interpolation of 3D morphology of faults.	39
Figure 2.25 Fault plane cutting the ignimbrite.....	40

Figure 2.26 Sketch showing the first model for the development	41
Figure 2.27 A fault with high vertical displacement but devoid of an opening.....	41
Figure 2.28 Schematic sketch of second model for the development faults.....	42
Figure 2.29 Determination of opening direction.....	43
Figure 2.30 Matching edges from cooling fractures.....	43
Figure 3.1 Map showing pyroclastic cones with their approximate alignment.	45
Figure 3.2 Volcano – tectonic map of the area	46
Figure 3.3 Tail cracks from Landsat images	47
Figure 3.4 DEM of south of Gedemsa.	49
Figure 3.5 Lava flow overprinting the pyroclastic cone.....	49
Figure 3.6 Basaltic flows	50
Figure 4.1 Highly altered pyroclastic material	52
Figure 4.2 Map with distribution of Thermal Vents.....	53
Figure 4.3 Fumaroles using for balneological purpose.....	54
Figure 4.4 Active Fumaroles.....	55
Figure 4.5 Fractures of Various sizes.	55
Figure 4.6 Map showing the interaction of structures and vent locations alignment.	57
Figure 4.7 Land Surface Temperature map of the area with Thermal Vents Distribution.	60
Figure 4.8 Onverlay map of Land Surface Temperature, Thermal vents and Lineaments.....	61

2. List of Tables

Table 2.1 Field measured fault length and throws.....	32
Table 3.1 Radiometric dates of rocks from Asella and Gedemsa areas.....	48

3. Appendices

Appendix 1. Field measured Fault Length and Vertical displacement (Throw).....	71
Appendix 2a: Kinematic measured data from Danisa area.....	72
Appendix 2b: Kinematic measured data from Salen/Artu areas.....	73
Appendix 3. GPS Locations of Active Thermal vents.....	75
Appendix 4. Radiometric dates of Main Ethiopian Rift and Afar	78

List of Abbreviations

EMA	Ethiopian Metrological Agency
DEM	Digital Elevation Model
ELC	Electro Consult
ASTER	Advanced Space borne Thermal Emission Reflection and Radiometer
UNDP	United Nations Development Program
EARS	East African Rift System
ER	Ethiopian Rift
MER	Main Ethiopian Rift
WFB	Wonji Fault Belt.
SDFZ	Silti – Debrezeit Fault Zone
GPS	Geographic Positioning System
LST	Land Surface Temperature

ABSTRACT

The Main Ethiopian Rift (MER) constitutes the northernmost part of the East African Rift System (EARS), connecting the EARS with the Afar triple junction and is an area characterized by active extensional tectonics and associated volcanic activities.

The area of investigation, Tulu Moye, is situated in the Main Ethiopian Rift (MER), northwest of Asela, close to the eastern margin of the rift. It is a wide zone where tectonic and volcanic activities are concentrated. The aim of this study is therefore, to show the relationships between extensional structures (normal faults and tensional fissures) and associated volcanic edifices with the aid of Geographic Information System (GIS) for compilation of available geologic, structural and thermal field investigations.

By integrating the Landsat images, aerial photographs and topo maps together with the field data the lithology and structures of the study area are mapped with better accuracy, minimum cost and shorter field seasons.

Volcano – tectonic data showed a close relationship between dense Quaternary faulting and associated eruptions. Volcanic activity is becoming more recent and young towards the central part of the area (west of the eastern escarpment).

Structurally the area is generally characterized by intense quaternary faulting and fracturing. Three set of faults are mapped in the area namely; NE – SW striking marginal normal faults, NW – SE to E – W trending trans-rift faults and the youngest and active NNE – SSW to N – S striking faults of the Wonji Fault Belt (WFB).

Almost flat foot wall and hanging wall tilted away from the fault plane is the typical morphology obtained from morphology data collected using Trimble GPS. An approximate E – W direction of extension is obtained from kinematic data collected at two selected sites.

Inventory of thermal vents in the area is made using Trimble GPS. The relationship between these thermal sites and tectonics of the area is clearly outlined. In such a way that, the vents follow the general NNE – SSW trend of the intensively and densely populated faults of the Wonji Fault Belt (WFB).

1. INTRODUCTION

1.1 Background

The Ethiopian Rift (ER) is part of the East African Rift System (EARS) and comprises a series of rift zones extending from the Afar triple junction at the Red Sea and Gulf of Aden intersection to the Kenya rift.

The Main Ethiopian Rift (MER) constitutes the northernmost part of the East African Rift System (EARS), connecting the EARS with the Afar Triple Junction and is an area characterized by active extensional tectonics and volcanism. The MER started to develop during Miocene time (Davidson and Rex, 1980; WoldeGabriel et al., 1990; Chernet et al., 1998) and it is also characterized by well developed Quaternary faulting that is mostly related to the Wonji Fault Belt, WFB (Mohr, 1967; Meyer et al., 1975; Boccaletti et al., 1998; Acocella et al., 2003). Despite the overall NE-SW trend of the MER, the WFB is characterized by active NNE-SSW trending extension fractures and normal faults, having an en-echelon arrangement and are associated with young volcanic activity.

The way in which faults influence subsurface fluid flow is important in many fields of Earth Sciences including Structural Geology. There is an increasing evidence for a close interaction between fluids and faulting (Hardbeck and Hauksson, 1999). Not only are fluids commonly driven to, and flow along fault zones, but also over pressurized fluids trigger slip in these zones (Hardbeck and Hauksson, 1999). But, the basic question regarding the relationship between fluid flow and fault hydraulic architecture remain unanswered.

Ethiopia has a significant amount of geothermal resources. This is due to the huge impact of the EARS which cuts through Ethiopia. Geothermal studies in Ethiopia date back to 1969. A regional reconnaissance work was conducted in the whole rift, including geology, geochemistry, hydrogeology and remote

sensing (UNDP, 1973). This work led to the selection of most promising areas, among which the investigation area, Tulu Moye, is one of the prospect.

Previous studies showed that the study area, Tulu Moye, is strongly affected by hydrothermal activities. The main hydrothermal manifestations in the area are weak fumaroles, active steaming grounds and altered grounds.

Many geologic investigations have been made in studying the lithology and structures in the region, but less has been done on detailed structural analysis of the area even though, it represents an area where the eastern margin of the Main Ethiopian Rift coincides with the WFB. This work is therefore, aims to conduct detailed structural characterization using computers and field surveys.

The area of investigation, Tulu Moye, is situated in the MER nearly close to the Eastern margin of the rift. This part of the rift is highly affected by WFB (Mohr, 1967). The study area is a wide zone where tectonic and volcanic activities are concentrated. The Eastern part of the area is affected by NNE-SSW trending closely spaced normal faults, local grabens and horst structures (Rift-in-Rift structures) and tensional fractures. In relation to the active extension, varieties of rift structures are formed (figure 1.2). This study also deals with the relationship between these structures, like normal faults tensional fissures, lava flows and volcanic edifices with their spatial relation to the various thermal manifestations in the area- Tulu Moye.

1.2 Geography

1.2.1 Location and Accessibility

The study area, Tulu Moye-Gedemsa, is located about 175km south of Addis Ababa in the central sector of Main Ethiopian Rift (MER). It lies between 500000-530000E and 885000-930000N UTM coordinates covering about 900km² (Figure 1.1).

The area is situated within the central sector of the Main Ethiopian Rift (MER) characterized by active tectonism and related volcanism. This part of the rift manifests faulted blocks with relatively steep scarps that form local horst and graben structures, long and narrow open fissures and cinder cones which constitute the very rough topography.

Eventhough, the area is bounded by two main Asphalted Roads namely; Nazreth- Asella and Mojo- Ziway, neither of them is helpful to reach the area. However, there are two dry weather roads both crossing the area, one from Kulumsa through Olgocho to Meki; the other from Dera to Haro Robi, which has been useful to access important geologic outcrops, structures and representative sites for this study.

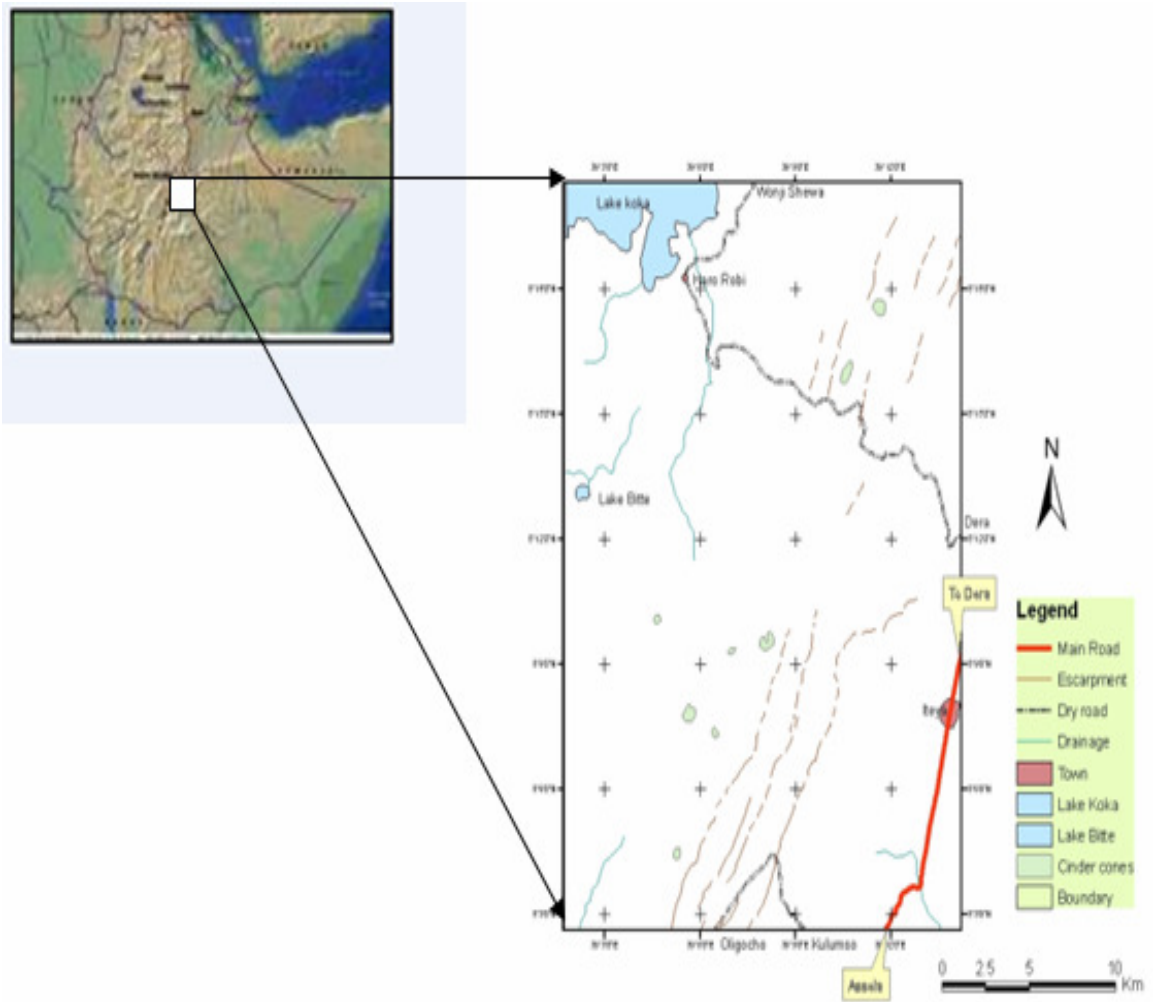


Figure 1.1 Location Map of the study area

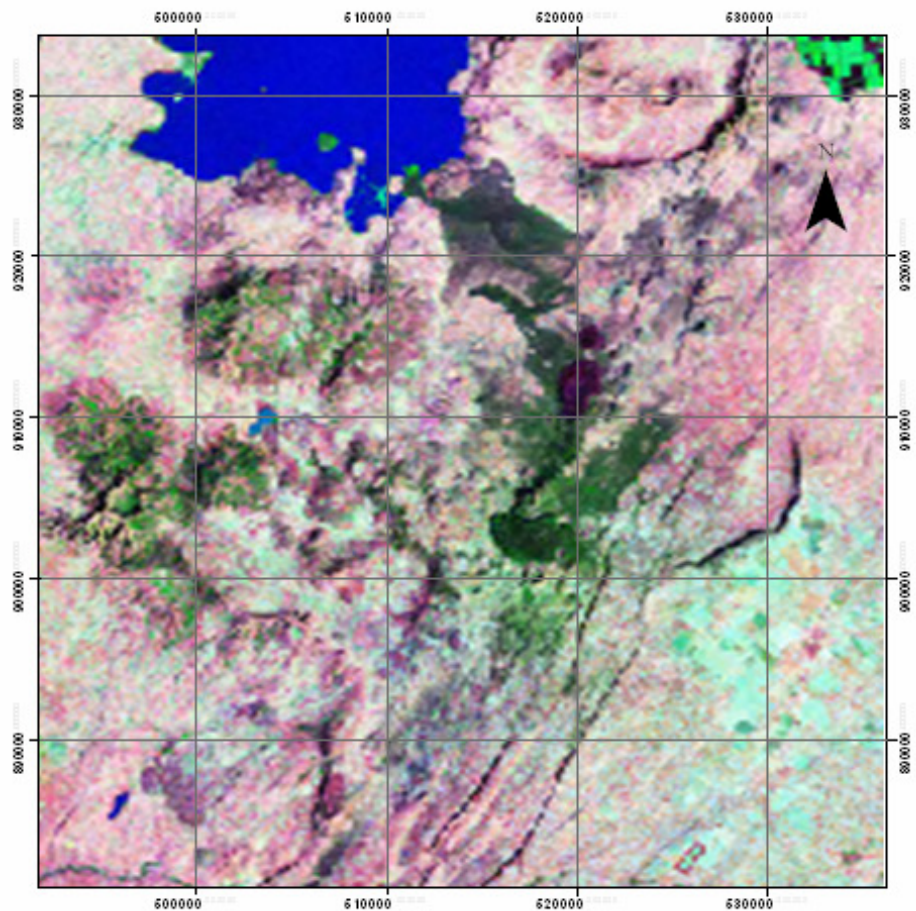


Figure 1.2 Study area from Landsat image. The distribution of different extensional structures like normal faults and volcanic edifices can be seen.

1.2.2 Physiography and Drainage

The study area is generally characterized by the occurrence of both mountainous and flat topography. Long and relatively narrow (1-5m) extension fractures (Tesfaye Korme et al., 1997), brecciated lava flows, lava domes, cinder cones, crater and calderas are the most notable features within the study area. The (Tulu Moye, Bora, and Berecha) localities represent the elevated topographies with altitude ranging from 2120-2266m above sea level. However, Asela scarp and Chilalo of altitude about 4000m is other topographical highs nearby the study area.

There are no perennial rivers crossing the area. However, wet season runoff from the mountains to the plains forms the seasonal lake called Bitte, in the central part of the area. The northern part of the area is actually bounded by Lake Koka.

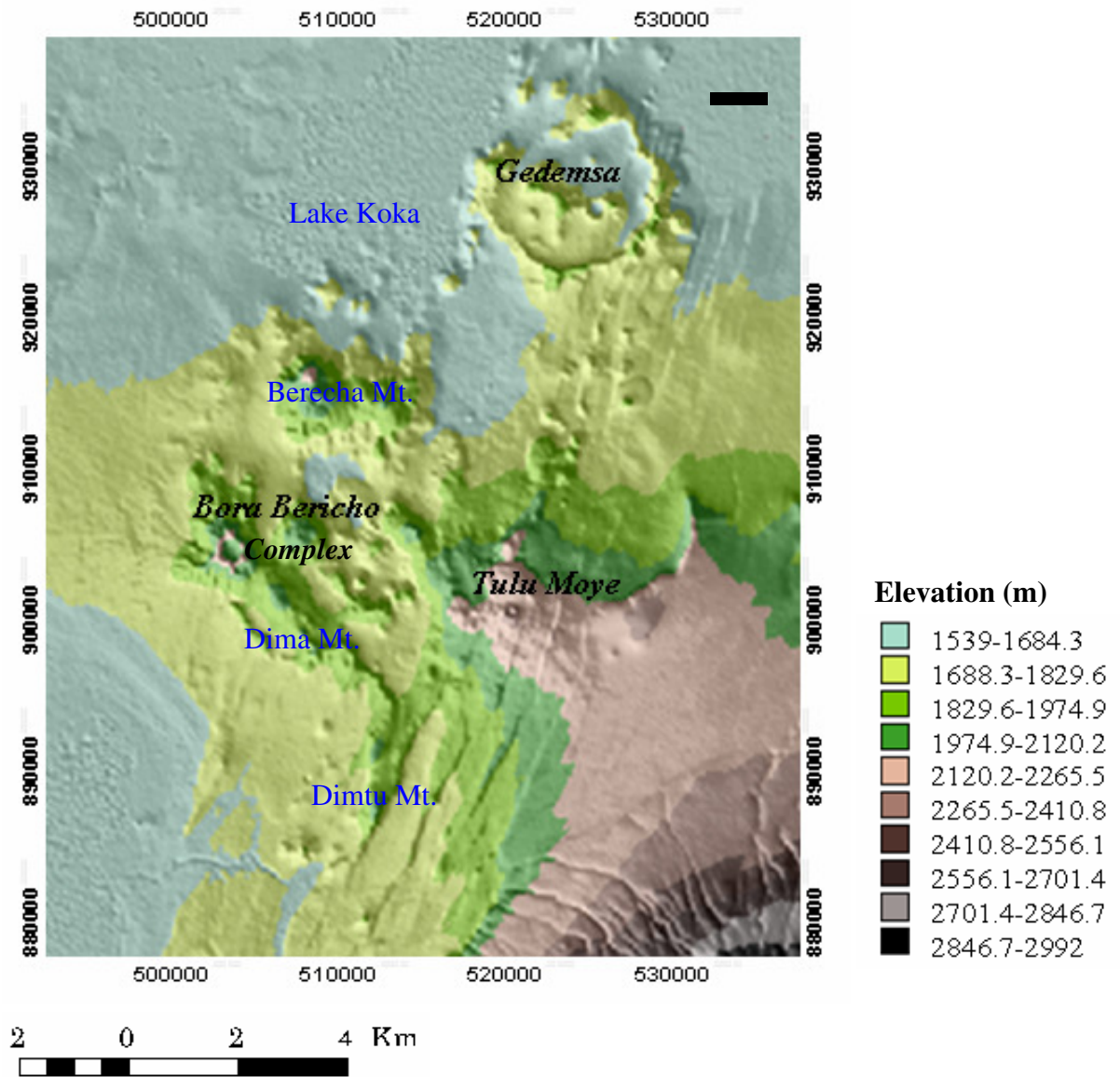


Figure 1.3 Topographic map of the study area from 3 DEM

1.2.3 Climate, Vegetation and Soil

According to Tesfaye Korme (1992), on the basis of the meteorological data collected from the meteorological stations at Ziway, Kulumsa and Awash Melkasa towns during 1989, the study area is classified into three main climatic zones. Namely, Temperate zone (Woina Dega), Warm zone (Kola) and semi- desert (Kefil Bereha) zone. Large portion of the study area falls within the Woina Dega climatic zone, having mean annual daily temperature of about 20°C. The area also receives rain fall during the rainy season mainly between June and September with mean annual rain fall of about 700mm/yr (EMA, 1988).

Eventhough, the study area is devoid of natural preserved forests, shrubs, acacia and short bushes are the dominant vegetation types in the area. The younger geologic activity in the rift valley has not permitted the development of soil horizons especially on pumice domes, scoria cones and rhyolite domes. As a result there are no big trees growing on these rocks. However, young rift floor basalt and obsidian flows are relatively better covered by thick vegetation.

The area is generally moderately populated. Peoples' lives depend on small-scale agriculture and cattle breeding. They grow corn, teff, barley and beans. Yellowish silty clay is the dominant soil type in the region.

1.2.4 Review of Previous Works

A large number of publications on the geology and volcano- tectonic development of the Main Ethiopian Rift in general, on the central sector in particular, have been produced in the past. These help to understand the regional geology of the studied area.

Many researchers have studied parts of the Main Ethiopian Rift such as Di Paola (1970) around Tulu Moye area, Gedemsa area and Kazmin and Seife Micheal (1980), Nazreth and northern MER. However, detailed structural analysis is not done, though the Tulu Moye area represents the Eastern margin of MER and is also a remarkable site where the NE striking border fault systems and the WFB system overlap to form the rift margin.

Di Paola. (1970) provided geologic descriptions of different rock types and geothermal conditions in the area and gave a brief description of hydrothermal areas in the lakes district.

WoldeGabriel et al., (1990) described the stratigraphic relations of the central sector of MER by using K/Ar dating of volcanic rocks from plateau escarpment and from the rift floor. From this stratigraphic framework and structural pattern of the area, they discussed the history of rifting and volcanism in the central sector.

Tesfaye Korme (1999) carried out lithologic and structural mapping of north east lake Ziway area, which included portion of Tulu Moye, with the help of Landsat TM data.

Electro Consult (ELC) with Geothermica Italiana and Ethiopian Institute of Geological Surveys jointly carried out a study during the year 1985-1987 under the project entitled “Geothermal Reconnaissance study of selected sites of the Ethiopian Rift System”. The purpose of the survey was to identify target areas for future detailed study to be carried out. With this aim, Tulu Moye-Gedemsa area was selected as one of the promising geothermal prospects in the Main Ethiopian Rift Valley.

Some geo- volcanological studies showed that, interesting geothermal features such as; occurrence of high concentration of recent volcanic flows, occurrence

of extremely active tensional tectonic features and widespread occurrence of altered and steaming grounds area common in the area.

1.2.5 Objectives

Generally, Tulu Moye is an area where the eastern margin of the Main Ethiopian Rift (MER) coincides with the Wonji Fault Belt (WFB) and also tectonic, volcanic and thermal activities are highly concentrated.

Eventhough, many geological investigations have been made in studying the lithology and structures in the region using conventional methods, detailed structural mapping and characterization with the aid of computer integrated field surveys and aerial photo interpretation is the first and primary objective of the research.

Specifically the objectives of this study are as follows:

- Conducting detailed geological and structural maps of the area.
- Constructing the possible inter-relationship between geologic structures and associated volcanism.
- To show the relations among geologic structures mainly lineaments in the area.
- Analysis of morphology, geometry and kinematics of fault systems.
- Make an inventory of thermal vents and observe how they are controlled by the fault systems.
- Analyzing the relation of volcanism, thermal manifestations and structures.

1.2.6 Methods and Materials used.

1.2.6.1 Methods

To achieve the above objectives, the study approach involves the steps outlined below:

1. Evaluation of Available data on the area

In the initial phase of the study, all existing information about the area to be studied is collected and evaluated. This includes analyzing topographic and geological maps at large (1:50,000) and small scales (1:250,000), reading and organizing all unpublished and published reports on geology, tectonics and thermal manifestations of the area. Further more, inventory of the Quaternary fault patterns and volcanic products, made from detailed interpretation of stereoscopic pairs of air photographs (1:50,000) and on screen digitization from Landsat imageries of 28.5m resolution are made to produce the tectonic and geologic map of the area.

2. Field investigations

Following the above analyses and interpretation of prior work, field investigations are designed to answer some specific questions regarding (a) identification of faults and volcanic edifices, interpreted from aerial photos and Landsat images in the field, (b) the morphology of Quaternary faults and fractures in the area, (c) the real interaction between the NNE striking faults/fissures and associated volcanic activities, (d) the distribution of thermal manifestations in the area and finally observing how these thermal sites clearly delineate the faults and fractures in the area are the basic tasks accomplished during the field work.

3. Post field work

All data collected during the fieldwork are further analyzed and processed by different softwares (ArcGIS, ERDAS, Geomatica, etc) in the office. In addition,

Interpretations of all computer output data, compiling and finally writing the report are also made in the office.

1.2.6.2 Materials used

The most common materials used in this study includes, softwares like ArcGIS 9.0, Arc View 3.2, ERDAS imaging, Geomatica, and Surfer to produce structural, geological and surface temperature maps. Especially Surfer is used for the 3D interpolations of fault morphologies and Trimble Business Center for conversion of GPS data to excel data. The materials used also include, tools like Trimble GPS to analyze fault morphology along and across the faults and fractures, hand held GPS, compass, hand-lens, geologic hammer, photo camera and others.

2. GEOLOGY

2.1 Geology of Ethiopian Rift

2.1.1 General geology

The Main Ethiopian Rift (MER) is part of the East African Rift System (EARS) lying within 5°00' and 9°00'N latitude and 37°00' and 39°00' E longitude (Mohr, 1967), Figure 2.1 (inset). The Main Ethiopian Rift is geographically divided into three sub sectors: northern, central and southern sectors (WoldeGabriel et al., 1990) and bordered by the Ethiopian plateau to the west and Somalia plateau to the east. The Main Ethiopian Rift, like the rest of the EARS, has undergone a very complicated geological evolution and tectonic history. Its geometry is characterized by normal step faults with orientation ranging from NNE-SSW to NE-SW (Mohr, 1967; Di Paola, 1977). The regional geology of the Ethiopian Rift System has been extensively described and well documented (Mohr, 1962, 1970). A simplified geological sketch map of the Ethiopian Rift, illustrating the major structural trends and location of rhyolite centers, is shown in figure 2.1 (After Kazmin, 1972). The rift valley was the site of extensive volcanic activities during the Tertiary. Volcanic rocks of Pliocene and Pleistocene age such as pantelleritic rhyolite, trachytes, ignimbrites and basalts are abundant within the rift floor and on the adjoining plateaus (Kazmin, 1972).

The oldest volcanic rocks, the plateau Trap Series, are exposed in the western escarpment and consist of basaltic lava with interbedded ignimbritic beds, overlain by massive rhyolites and intervening tuffs and basalts (Di Paola, 1972; Merla et al., 1979; Woldegebriel et al., 1990). Radiometric ages range from 40 to 25 Ma in the basalt and from 37 to 27Ma in the Rhyolites (Merla et al., 1979; WoldeGabriel et al., 1990). Middle Miocene to Pliocene (15-3Ma) basalt flows, rhyolites and tuffs unconformably overlie the early Tertiary volcanic units (Merla et al., 1979; WoldeGabriel et al., 1990).

The eastern margin is covered by Pliocene to early Pleistocene (4.6-1.6Ma) shield volcanoes (Chilalo, 4005m; Kekha 4245m; Badda, 4170m). These consist of trachytes with subordinate basalt (Di Paola., 1972; Merla et al., 1979; WoldeGabriel et al., 1990; Bigazzi et al., 1993). Silicic pyroclastic materials cover most of the MER floor (Mohr, 1962; Di Paola, 1972; WoldeGabriel et al., 1990); they are Early to Middle Pliocene (4.2-3Ma, WoldeGabriel et al., 1990), mainly peralkaline rhyolitic ignimbrites interlayered with basalts and tuffs. Alkaline and peralkaline rhyolitic lava flows and domes associated with pumice and ash represent the late silicic volcanic events (Di Paola, 1972). These lavas were erupted from late Pliocene to middle Pleistocene.

A more recent volcanic unit outcrops along the Silti-Debre Zeit Fault Zones (SDZfz) and the WFB (Di Paola, 1972; Kazmin et al., 1980); it is made up of basaltic lava flows associated with scoria cones. It is very recent as testified by radiometric ages of 0.13Ma (WoldeGabriel et al., 1990). Young volcanoes and calderas, such as Bora Bericcio complex, the Aluto volcano and Corbetti calderas, are made up of rhyolitic lava flows, unwelded pumice flows and ashes. Obsidian flows represent the final products of the volcanic activity (Di Paola, 1972). These recent volcanoes started to be active from the middle Pleistocene (about 0.25Ma, Di Paola, 1972; Mohr et al., 1980; WoldeGabriel et al 1990).

The Precambrian rocks in Ethiopian Rift System, except in the northern Afar and at the extreme south of the Ethiopian Rift, are mostly covered by more recent Tertiary volcanic rocks and Mesozoic sediments (Mohr, 1962). However, there are windows of metamorphic basement rocks of Precambrian age and Mesozoic sedimentary rocks in a few localities. These pre-Tertiary rocks are exposed along the eastern, western and southern Afar margins. Limited outcrops of Precambrian rocks covered by Early Mesozoic fluvial sandstones, marine shales and limestones, occur along the western margin of

central sector of the MER at Kella Horst and at Amaro Horst, in the southern sector of the MER (Lavitte et al., 1974; Zanettin et al., 1978).

Generally, WoldeGabriel et al., (1990) subdivided the volcanic products of the whole Ethiopian Rift into six main tectonomagmatic chronozones since Eocene to Oligocene. The description is adopted from this work as follows:

2.1.1.1 Kella Basalt: this is the oldest volcanic unit in the central sector of MER and is found at Agereslam, Ambo and Kella. These rocks are dominated by basalt with localized rhyolite and sedimentary strata.

2.1.1.2 Shebele Trachyte: the rocks of this unit are exposed along some deep canyons of Omo River and the Wabi Shebele. This group is dominated by intermediate and acidic volcanic rocks such as trachyte, phonolite, rhyolite and intercalated volcanoclastic strata.

2.1.1.3 Guraghe Basalt: Basalts and subordinate silicic flows of this unit are found at Awasa, Guraghe and Omo river canyon. In Omo river canyon, these 10.6Ma old basalts are underlain by several undated basalt flows and Middle Miocene Shebele trachytes. At Awasa and Guraghe, the base of correlative units is not exposed.

2.1.1.4 Butajira Ignimbrite: Voluminous silicic pyroclastic material and subordinate basalt flows of this unit were erupted from the Awasa caldera, the Wegebta caldera complex and a major caldera probably buried beneath the Ziway- Langano- Abijata basin. Petrologically these groups of rhyolitic rocks are distinguished from those of the Quaternary Wonji Group as being transitional or mildly peralkaline while the Wonji Group is peralkaline.

2.1.1.5 Chilalo Trachyte: This group includes the product of Pliocene centers of the eastern and western shoulder of the rift and compositionally correlative units from the Awasa caldera. It includes trachyte, silicic rocks and basalt that overlie units of either Shebele trachyte or Butajira Ignimbrite.

2.1.1.6 Wonji Group: This group is generally confined to the Wonji Fault Belt (WFB), along the entire MER and also includes the young basalts of SDZFFZ.

This group consists of the diverse Quaternary lava, pyroclastic rocks and volcanoclastic strata younger than 1.6Ma.

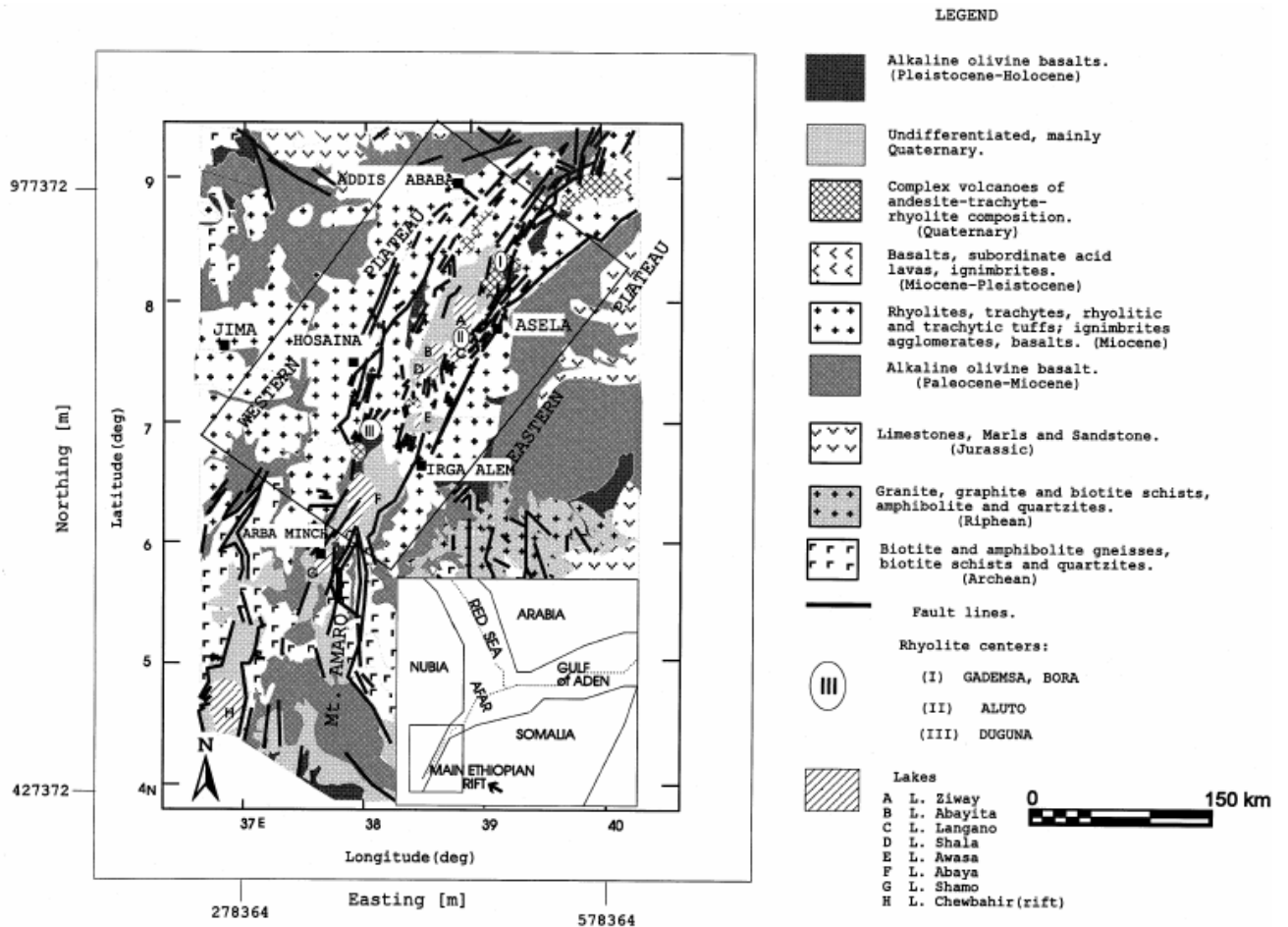


Figure 2.1 Geological sketch map of the Main Ethiopian Rift (MER). After Kazmin, 1972)

2.1.2 Structural Framework of Main Ethiopian Rift (MER)

The East African Rift System (EARS) is one of the largest continental rift systems on the Earth which provides an opportunity to investigate the compositional variation of erupted magma with the amount of extension. The East African Rift System is a Miocene- Quaternary intracontinental extensional system, divided into Eastern and Western branches and composed of several interacting segments from Mozambique to Afar (Davidson and Rex, 1980). At Afar, the East African Rift System joins the Gulf of Aden

and Red Sea Rifts, both characterized by a more advanced extensional stage (McKenzie et al., 1970; Ebinger and Hayward, 1996).

The Main Ethiopian Rift (MER) constitutes the northernmost part of the EARS, which represents an example of a young continental rift at an incipient stage connecting the EARS with the Afar triple junction. The main Ethiopian Rift started to develop during Miocene time (Davidson and Rex, 1980; WoldeGabriel et al., 1990; Chernet et al., 1998). During Pliocene and Quaternary, the MER progressively deepened, evolving through a sequence of interacting half- graben segments marking the boundary between the Nubia and Somalia plates (Hayward and Ebinger, 1996). The MER is limited by discontinuous boundary faults, active from Miocene (WoldeGabriel et al., 1990). Based on structural features, the MER is subdivided into southern, central and northern sectors.

In the MER two main distinct fault systems are recognizable: the older includes a NNE-NE trending steep, segmented Miocene rift bounding border fault system which is well developed especially along the Eastern margin separating the rift zone from the Somalia plateau. The younger includes Quaternary N-NNE trending right stepping en echelon fault system, which is considered as the axial zone, the youngest part of the rift that presently coincides with the Wonji Fault Belt (WFB). The WFB is located between the rift borders and affects the rift floor branching off from the eastern border. According to Meyer et al., (1975), the WFB faulting started developing at the beginning of the early Pleistocene (~1.6 Ma ago). Despite the overall NE- SW trend of the MER, the WFB is characterized by active NNE- SSW trending extension fractures and normal faults, which in many places are associated with fissural and central volcanic activity (Gibson, 1969; Mohr, 1987; Chorowicz et al., 1994; Korme et al., 1997). The normal faults are in most cases arranged in a right stepping en echelon configuration (Mohr, 1968; Boccaletti et al., 1998) and the vertical throws are in the order of several tens

of meters (in the axial zone; Gibson, 1969) to several hundreds of meters (in the margins; Hayward and Ebinger, 1996).

Figure 2.2 is lineament map interpreted from Landsat image of resolution 28.5m, Aerial photographs and topographic maps of scale 1:50,000 and from recent study (Abebe et al., 2007). The map shows the spatial geometrical relationship between marginal and rift floor normal faults and minor extension fractures. However, minor lineaments less than the resolution of the system are not detected and mapped.

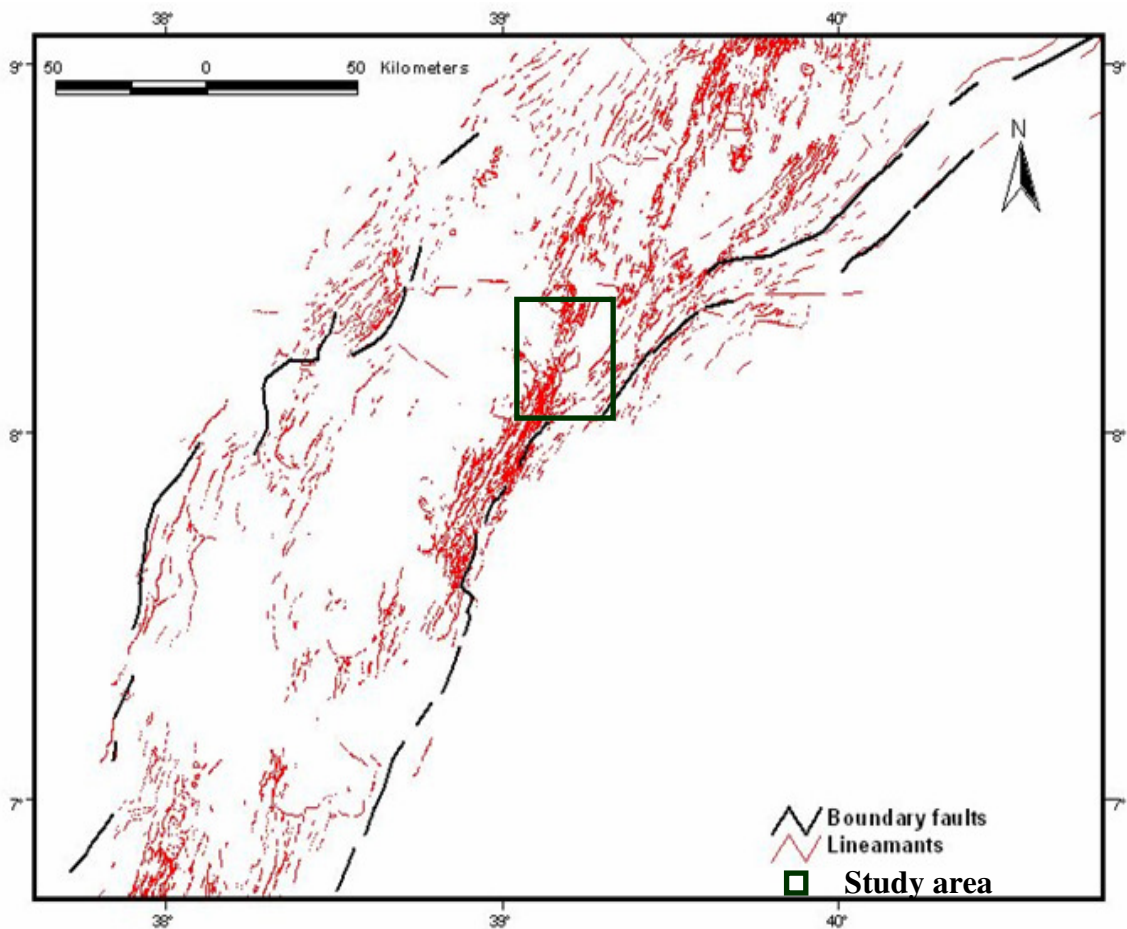


Figure 2.2 Lineament map across the MER between 7°N and 9°N. Extracted from Landsat image aerial photos and topographic maps and (Abebe et al., 2007).

2.2 Geology of the Study Area

2.2.1 Lithology

The geological map of the area is produced (figure 2.8) mainly from earlier geological maps of Lake Ziway-Asela and Nazareth-Dera regions (Alula et al., 1990; Abebe et al., 1998), recent studies (Abebe et al., 2007; Bocaletti et al., 1998), and interpretation of Landsat TM with field observations. The map is presented in broad sense. For example, the western part of the area is mapped broadly as pantelleritic pumice fall and lava domes, but many lithologies like rhyolites, lava domes and pumice falls are contained in it. The following geologic units are accessed and identified in the studied area; the discussion from the oldest to the youngest is as follows:

2.2.1.1 Pantelleritic ignimbrite and unwelded tuff

Ignimbrites of Nazareth group are exposed in the mapped area. This unit covers large area in the southeastern and southern end of the studied area forming scarps due to faulting. The maximum thickness of this unit has been found along the main boarder fault escarpments, south west of Kulumsa village. It consists of pantelleritic and commendite ignimbrites exhibiting different textural characters due to the grade of welding. The only radiometric age available on this product is of 1.66Ma (WoldeGabriel et al., 1990). However, relatively younger Holocene ignimbrites are also mapped in the northeastern part of the area. This unit consists of ignimbrites and minor lava domes and flows related to caldera collapse. It usually overlies the Asela unit and consists of peralkaline rocks. These units are both generally characterized by poorly welded, more or less fresh with different lithic fragments, like pumice and basalt.



Figure 2.3 Relatively weathered ignimbrite with fresh pumice and basalt interlayers.

2.2.1.2 Basalts

This is also a broad division including recent rift floor scoriaceous basalts and relatively older porphyritic basalts of Tulu Moye.

The fresh rift floor basalts cover the northern Artu southeastern Gedemsa areas. This basalt is generally of aa type and outpoured through NE trending open extension fractures. Petrographically it is composed of abundant plagioclase with some pyroxene and olivine.

Relatively old porphyritic basalts are also the thickest and widely distributed basalt type exposed in whole thickness around Artu area. This unit covers larger area in Tulu Moye (central part of the mapped area) and wider areas in Deneba and Danisa localities.

This basalt is generally of pahoehoe type and as indicated in the geological map it is usually outpoured through recent NE trending open faults. Its groundmass is characterized mainly plagioclase lathes and glass.

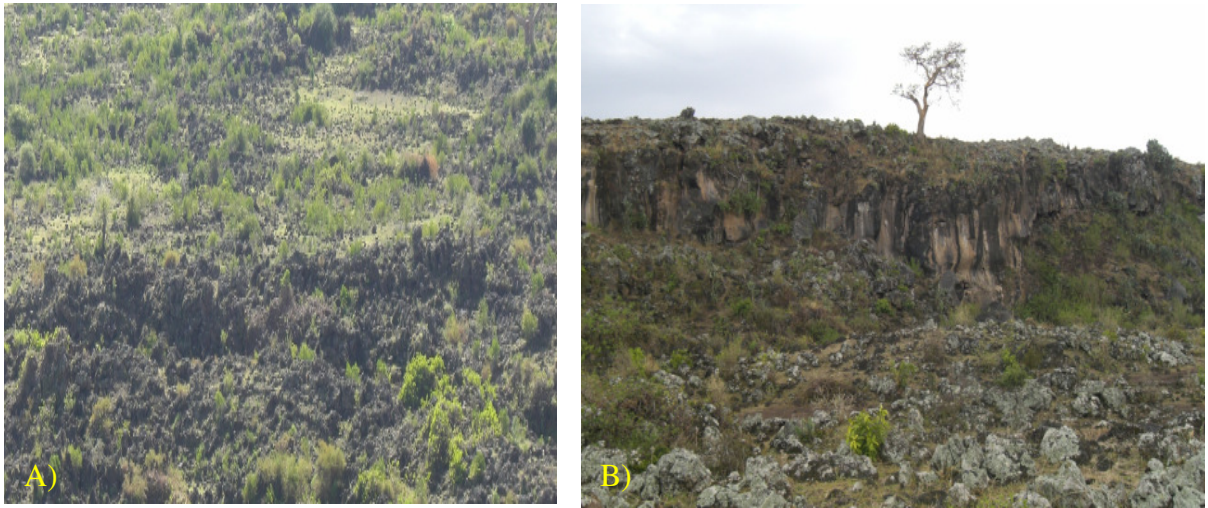


Figure 2.4 AA and pahoehoe type basalts outpoured along active extensional fractures and major faults in Shenen and Deneba areas, A and B respectively.

2.2.1.3 Pyroclastic Cones

This unit is generally located in the tectonically and magmatically active graben and horst structures, extending from south to north of the mapped area. As shown in the figure 2.5 most pyroclastic cones are found mainly on basalts (Tulu Moye and rift floor basalts). However, some pyroclastic cones are situated on the ignimbrites and unwelded tuffs of eastern and southern parts. This unit in the area seems to be older than the lineaments (normal faults and fractures) and recent obsidians and basalts erupted through fissures/fractures.



Figure 2.5 Pyroclastic cone consisting of loose to welded lapillis

2.2.1.4 Obsidians, Trachytes and Lava domes

Generally this is a broad category including all the varieties of glassy obsidians, lava flows and trachytic domes.

Obsidians and lava domes are mapped on the central and northern part of the area, clearly outcropping at Artu and south of Gedemsa, respectively. Whereas trachytic rocks, in the area occur in the form of sheet flows and moderate mushroom shaped lava domes. They are concentrated in the western and eastern parts of the mapped area.



Figure 2.6 Obsidian dome consisting of massive obsidian flow (A) and mushroom shaped trachytic rocks, east of Shenen (B)

2.2.1.5 Alluvials deposits

There are also sedimentary units, which cover the lower depression of the rift. Specifically, this unit blankets the top of volcanic rocks of the graben. This unit contains fine ash, sand and clay deposit and currently used for agricultural purpose.



Figure 2.7 Hanging wall covered by alluvial deposit, Deneba area

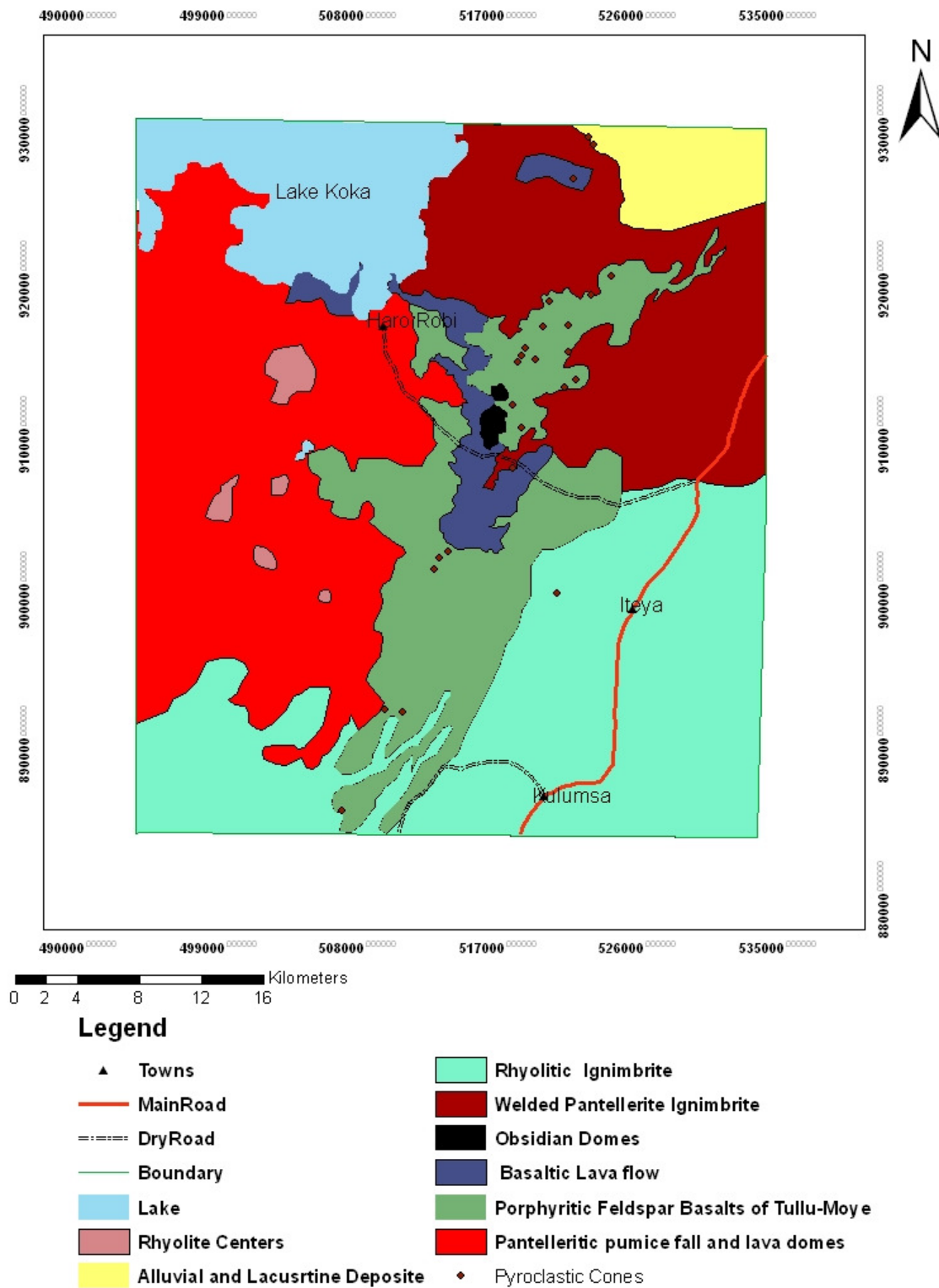


Figure 2.8 Geological map of the study area. (Extracted from Landsat image, Nazreth geological map (1:250,000) and geological map of lake Ziway – Asella region (1:50,000))

2.2.2 Structural Interpretation of the Area

The Photo- interpretation of faults is often more reliable than their detection in the field. Because fault surfaces are rarely seen at outcrops and change in vegetation and surface texture related to faults are difficult to see at close range. Stereoscopic viewing enabled to see more subdued topographic features and reveals clearly vertical displacement associated with faulting. In the structural map (figure 2.10), the graben and horst structures are therefore, clearly mapped from photo interpretations supported by field surveys at the scale of 1:50,000. In the central, northern and southern part of the area, which is highly affected by the Wonji Fault Belt (WFB), the rift-in-rift (graben- horst) structures usually run parallel to each other. Lineaments (faults and associated tensional fissures) are relatively concentrated on the eastern part of the area closer to the main eastern escarpment of the rift valley. The direction of downthrow of the faults is again variable but more commonly to the west associated with tensional fractures.

Generally, from landsat TM image, topographic maps and aerial photo interpretations supported by field observations, three major fault sets are identified in the studied area:

1. NE – SW to NNE-SSW rift boundary faults

These are oldest boundary faults that fall in the study area and usually found north of Ogolcho and southeast of Iteya towns. NE-SW striking boundary fault at southeast of Iteya is persistently similar to the eastern rift marginal faults found on the plateau whereas the boundary fault at north of Ogolcho is characterized by having a trend of NNE-SSW. These faults are characterized by high vertical displacements and NW down throw directions.

2. NW – SE to E – W Cross – rift faults.

Mapping the cross rift faults in the area from integrated interpretation of aerial photos and landsat images is the other interest in this study. These faults are found rarely in the area. In Bora Bericho NE-SW trending cross rift faults are mapped. As shown in figure 2.10, these faults are branching from

NNE-SSW trending Wonji Fault Belt, implying that they are almost of the same age. The southern tip of the study area (Dimtu Mountain) is characterized by almost E –W striking cross – rift structures which are usually interrupted or cut by the later coming younger faults and fractures (figure 2.10). Previous studies showed that, in some localities outside the area such as northern boarder of Lake Ziway, Ketar and Meki Rivers followed these trans rift structures (Tesfaye Korme, 1999).

3. NNE – SSW and N – S youngest normal faults.

The youngest faults in the area are those striking N-S to NNE-SSW, which covered larger areas in the northern, central and southern parts of the study area. These faults are generally normal step faults with down throws up to 30m to the west as well as to the east. The faults mainly form rift- in- rift system of structures that run tens of kilometers parallel to each other. Some of the surveyed grabens are occupied by younger basaltic flows extruded from the fissures and partially being filled by alluvium.

These faults usually cut recent porphyrtic basalts, obsidian & rhyolite domes and pumice & scoria cones. Some of them have got very small throws but are probably deep penetrating. Fractures/fissures with wide opening but devoid of vertical displacement are also mapped together with NNE trending faults. The eruption of the youngest basalts and acidic lavas, such as rhyolite and obsidian domes seem to be controlled by these faults. It is generally assumed that, these faults resulted from intensive tensional stress associated to the normal faulting.

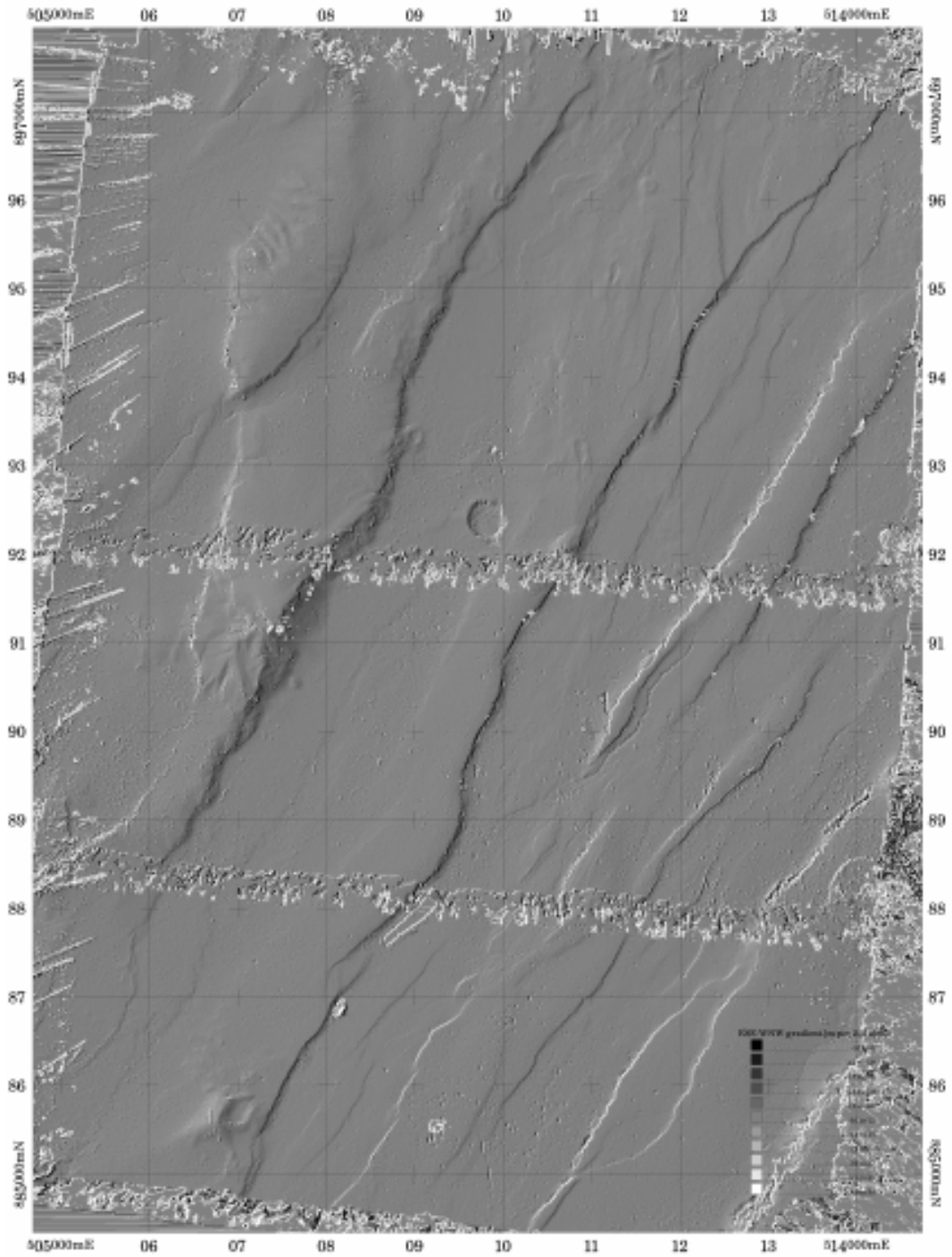


Figure 2.9 DEM of southern part of the study area, Deneba and Danisa.

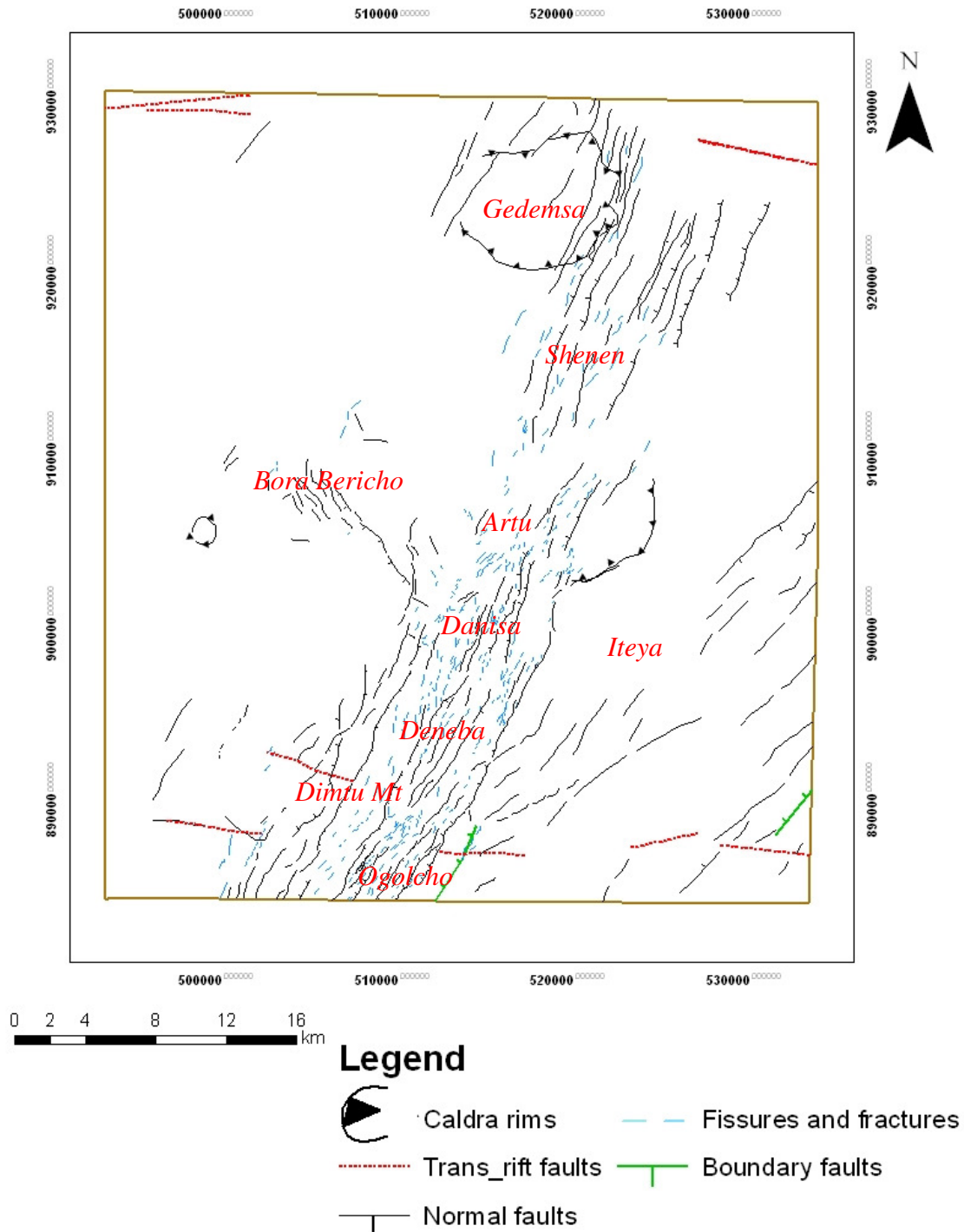


Figure 2.10 Tectonic map of the study area. Extracted from Landsat image, Aerial photos, Topo maps and Field surveys

2.2.2.1 Fault Morphology

The pattern of faulting consists of several narrow grabens and horst structures. Fault Morphology surveys are made in the southern and central parts of the area at Deneba, Daluta, Tero/Salen and Danisa areas. In Deneba and Danisa areas, clear flexural faults are observed in the basaltic field and have typical fault behavior. Morphologically, these faults are characterized by steep and high escarpments (5-25m) at the centre and change in to simple fractures along strike or die out.

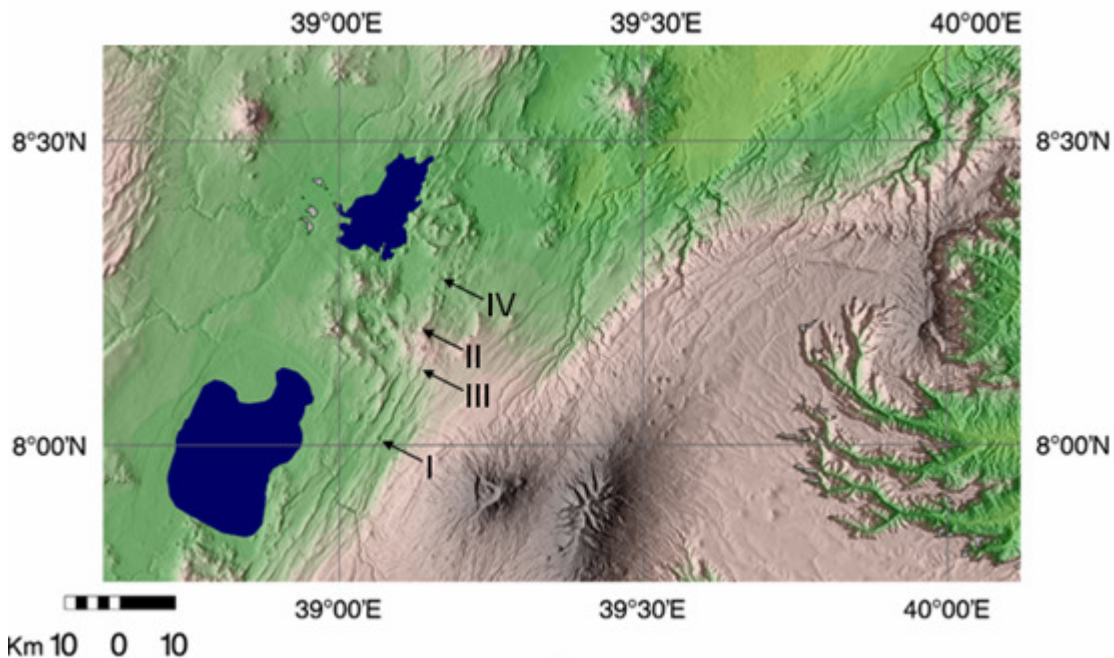


Figure 2.11 ASTER image showing sites of fault morphology survey: I) Deneba, II) Tero/Salen III) Danisa IV) Daluta

Morphology data were collected in the selected sites using Kinematic Trimble GPS usually on profiles across and along the faults (figure 2.12 and 2.13). From these data, 2D cross-sections of selected profiles across faults are prepared, which indicate that, most of the faults do not show the morphology of typical flexural faults. Rather they attained morphology of relatively flat footwall and hanging wall tilted away from the fault plane.

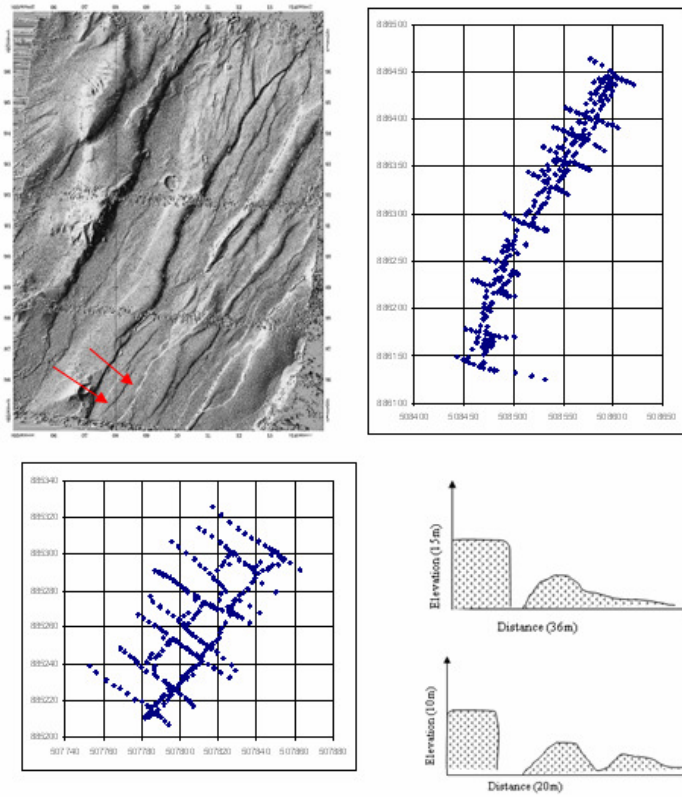


Figure 2.12 Fault morphology profiles and cross section from field observation across a fault, Deneba area.

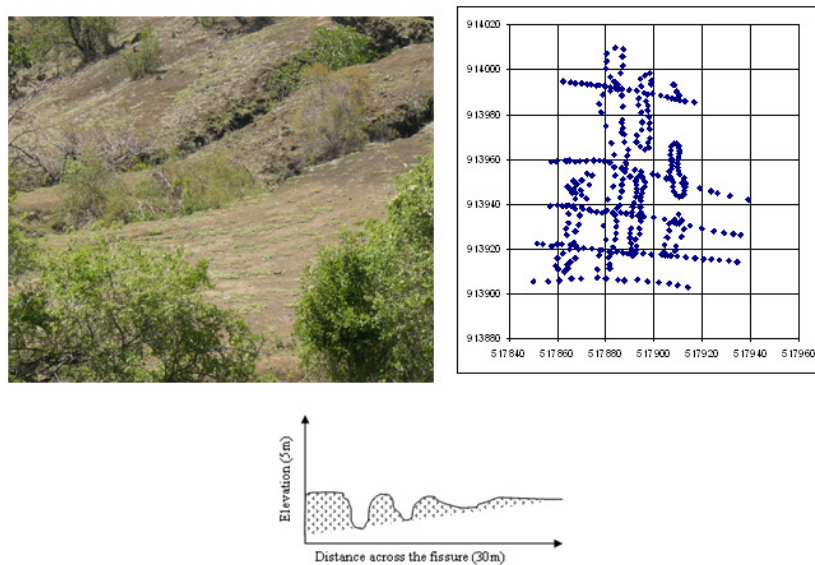


Figure 2.13 Fissure morphology profiles and cross sections from field observations across a fault, Daluta area.

However, in the northern end of the study area (Shenen and Lugo) fault behavior changes in different geologic materials. In these areas, for example two distinct fault morphologies are clearly observable following different geologic units. Massive lava flows and pyroclastic materials are the two typical geologic units where change in fault morphology is noticeable. In massive lava flows or welded ignimbrites, faults exist as steep and high escarpments. A lithological change to a loose pyroclastic material results in a step back of the fault and lower scarps. In many cases, the faults die out when the material changes to pyroclastic material that means the fault is not visible any more. It seems the thinner the lava flow the lower the escarpment, because in the middle of a flow relatively the highest escarpment up to 20m is observed (Figure 2.14)



Figure 2.14 Morphology of the fault change along its length. On the right side, the fault shows a gently dipping scarp because it cuts through the pyroclastic material of cone 1. In the central part it steepens and it has the highest scarp within the middle of the lava flow. The lava flow thins out towards the cone 3 to the left and the fault dies out within the pyroclastic cone. View from west to east.

There are typical forms of fault tips depending on the material in which the fault ends. When the fault dies out within pyroclastic material at the end of the lava flow, the escarpment gets less and less until it is only a small flexure.



Figure 2.15 Both faults are dying out at the cones consisting of pyroclastic material. The highest escarp of the faults cut through a massive lava flow, which is getting thinner towards the cones, equivalent to the morphological change of the fault escarpment. View from southwest to northeast.

2.2.2.2 Formation and Growth of Faults in the study area

Normal faults are commonly well developed features in rift zones. Among these, active narrow rift zones are characterized by a focused area of extension and offer the opportunity to observe within a limited area, normal faults at different stages of evolution (Buck, 1991).

Rift zones are made up of several interacting extensional segments (Bonatti, 1985; Ebinger et al., 1987; Gudmundson, 1992; Nelson et al., 1992; Hayward and Ebinger, 1996). At the early stages, these usually consist of half graben like structures, interacting and evolving towards symmetry and turning in to graben like structures at latter stages (Ebinger et al., 1984; Bosworth, 1985;

Gudmundson, 1987a; WoldeGabriel et al., 1990; Kazmin and Byankou, 2000). Regardless of these symmetries, a narrow rift shows an inner younger and active zone of extension characterized by subparallel extension fractures and normal faults, whose vertical displacement increases from the axial zone towards the mature rift margins (Mohr, 1968; Needham et al., 1976; Tamsett, 1986; Martinez and Cochran, 1988; Forslund and Gudmundson, 1991, 1992; Angelier et al., 1997). It is accepted that subparallel extension fractures and normal faults form contemporaneously and independently under the same stress conditions in the axial part of a rift (Gibson, 1969; Pollard et al., 1983; Tamsett, 1986).

So the aim of this section is to show how normal faults in the area are formed and what is their real interaction or relationships between the associated extension fractures.

Field analysis was carried out in selected sites of the study area, namely the northern (south of Gedemsa) and southern tip (Deneba), which are characterized by abundant extension fractures and normal faults. Field data collection included mapping and measuring the geometry such as (length, strike, dip) and kinematics such as (dilation, throw, extension direction and hanging wall tilt) for more than ten normal faults and fractures.

According to the data collected on these sites, the active normal faults observed show proportional relationship between their length and throw (Table 2.1). These implied, the longer the faults, the larger the vertical displacement they attained or larger displacements are associated with longer faults indicating interdependence between the horizontal and vertical dimensions of the faults.

Table 2.1 Field measured fault length and throws.

No.	Fault length (m)	Vertical displacement (m)
1	2160	25
2	2000	23
3	1800	20
4	1500	15
5	1300	12
6	1100	10
7	800	8
8	600	6
9	500	4
10	400	2
11	200	0

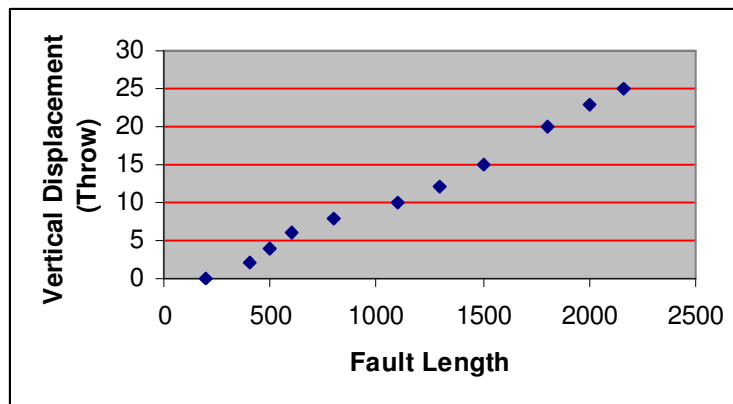


Figure 2.16 Normal faults showing a direct proportion between their lengths and their throws.

Most of the observed Quaternary normal faults responsible for extension show throw larger than a meter with significant opening. Vertical walls, suggesting a sub vertical geometry for the faults at the surface, border these open normal faults (figure 2.17). The layers in the hanging wall regularly show a tilt, usually between 10° and 45° towards the downthrown side.



Figure 2.17 View from north to south shows an open normal fault with vertical wall and tilted hanging wall.

Previous studies on the normal faults on the axial zone of Ethiopian Rift showed that, the openings of the normal faults in the axial zone tend to be proportional to the throw of the faults either along the same fault or in different faults. However, in the studied area, this is not the case observed in such a way that, the relatively older and well developed faults are devoid of these openings. Actually relatively young faults proved the proportionality of openings and throws along the same fault.

Based on this idea, generally three stages of faulting have been observed in the studied area:

1. The faults, which are symmetrical on both east and west sides running with an approximate strike of $N30^{\circ}E$. These faults are on welded ignimbrite

and have a maximum vertical displacement of about 25m. Most of these faults lack openings, but few attain openings of not more than 4m. Based on field observation, these faults are generally interpreted as mature faults that completed their phase of faulting.



Figure 2.18 Relatively matured fault with out any opening. View from east to west.

2. There are also faults within welded ignimbrite, running with an approximate strike of N25°E and having significant vertical displacement but less than the above faults. However, these faults have got openings up to 6m and accompanied by branching fissures and fractures from them. The tips of these faults terminate as a fissure having typical morphology with dipping monoclinical hanging wall.



Figure 2.19 The arrow shows a fault with tilted hanging wall and significant opening

3. The third type of faults are simple fractures and fissures most of which lack vertical displacement, running at approximate strike of 10°-15°NE and placed at the centre of the basaltic field. These faults attain a maximum opening of about 10m, through which either basalts are erupted in areas like Deneba or are filled by latter coming lava flow as in south of Gedemsa area.



Figure 2.20 Arrow showing deep open fissure in Deneba. View from east to west

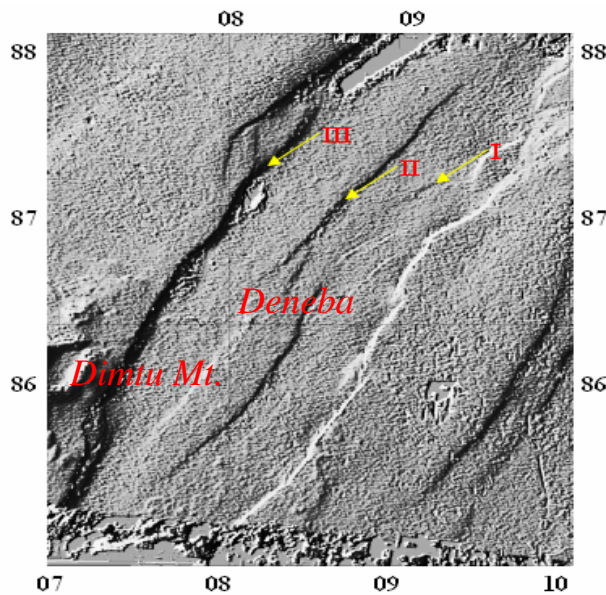


Figure 2.21 Map with the three phases of faulting. Details see above.

A further feature of normal faults in the area is their common association with extension fractures. There is no significant development of minor extension fractures subparallel to normal faults along the foot wall and the hanging wall of normal faults. Nevertheless as for example in Figure 2.22 below, extension fractures often branch from normal faults or replace limited parts of them. In particular, the throw of normal faults regularly decreases at the tips and the faults terminate as a sub vertical extension fractures, which also regularly decrease in their opening (see figure 2.23). Moreover, for example figure 2.24 shows an observation made on a single fault segment at Deneba area. Along this segment both fissure and fault are observed with clear transition of monoclininal fissure to normal fault. The collected data generally suggest that, the normal faults nucleate from simple extension fractures with clear and observable transition zone.

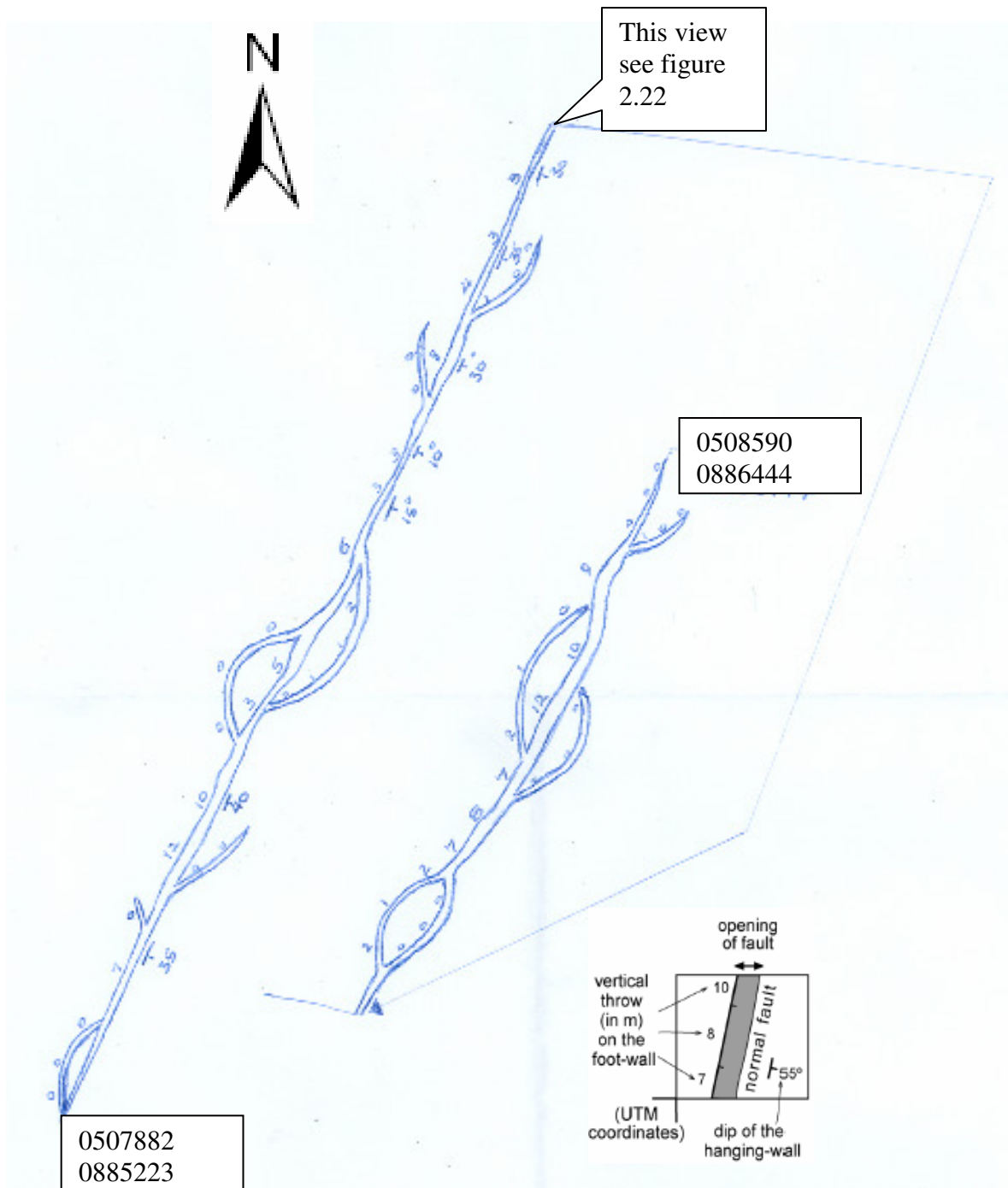


Figure 2.22 Field sketch map of a representative open normal fault observed in welded ignimbrite. Deneba area. Numbers on the foot wall indicate vertical displacement in meter. See inset (after Acocella, V., and Korme, T., 2002). Not to scale.

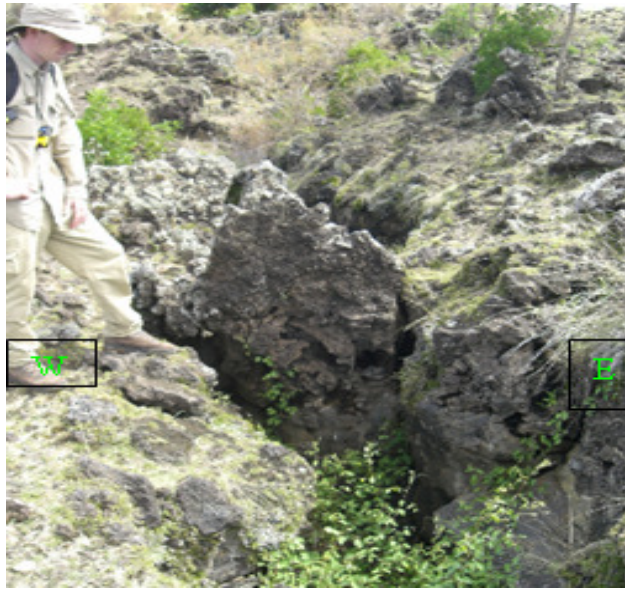


Figure 2.23 This view from north to south shows termination of a fault, open fissure

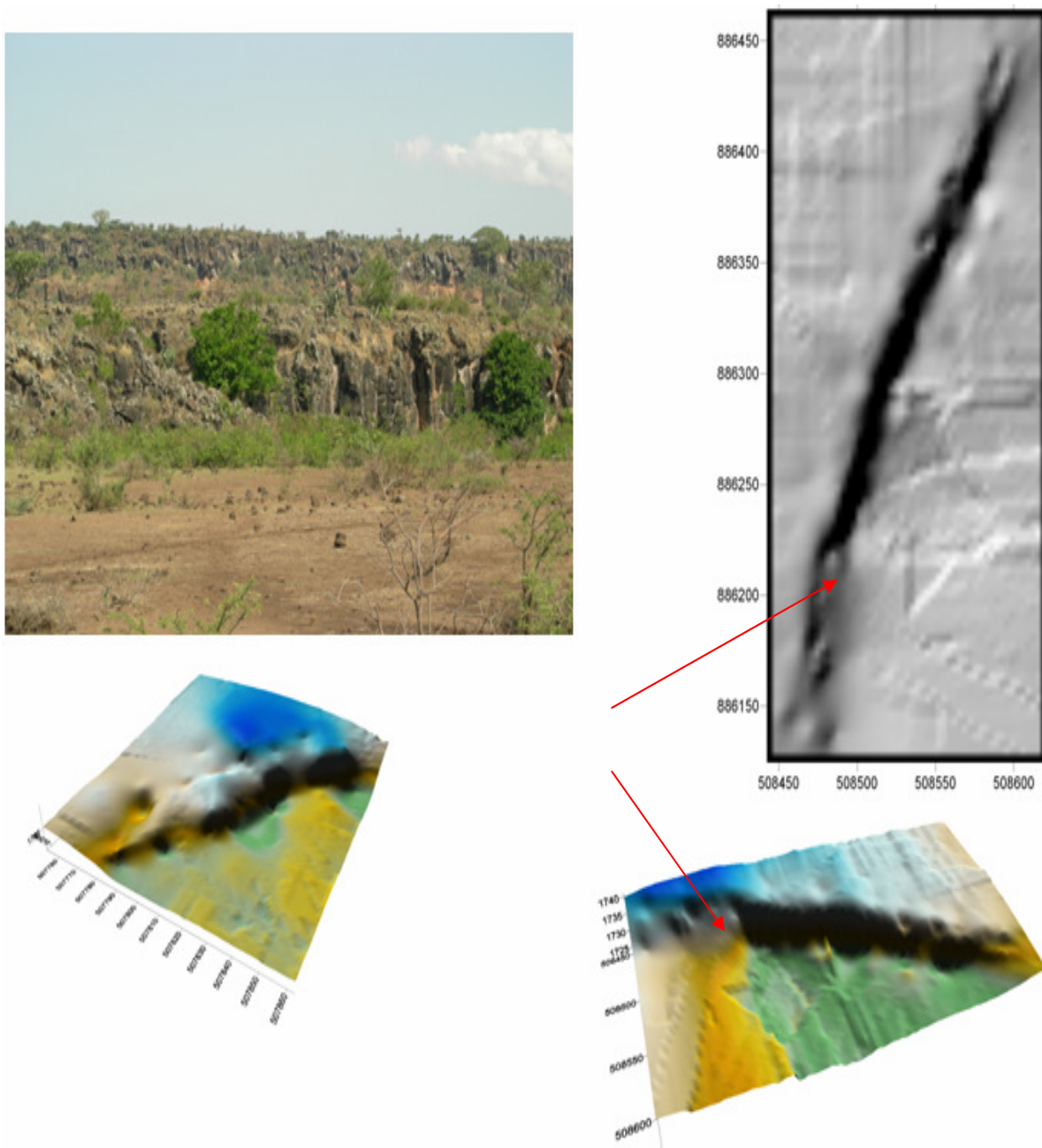


Figure 2.24 Interpolation of 3D morphology of faults using Surfer. The arrows indicate the transition of monocline fissure to normal fault.

2.2.2.3 Fault Models

Based on field observations on faults and fractures, the study generally proposed two different types of fault models in the area.

The first model is therefore, proposed for most of the extension fractures and normal faults of about 5-10m high fault scarps with significant openings, covering large part of the study area. For example, figure 2.25 is a 10m high fault scarp where a basaltic flow is overlying an ignimbrite. The basaltic flows either on the foot wall or on the hanging wall are of the same type and age. Both layers (basalt and ignimbrite) are cut by the fault plane and several slabs of basaltic lava covering the ignimbrite are on the fault plane. From this observation, it is concluded that, there had to be at least a fissure in the ignimbrite during the eruption of basalt, so that the basalt can flow through it. Therefore, this model suggest that, first extensional fissure generate through which the basalt erupts and latter they get a vertical displacement.



Figure 2.25 Fault plane cutting the ignimbrite have been buttered by basalt. View from West to East. Deneba area.

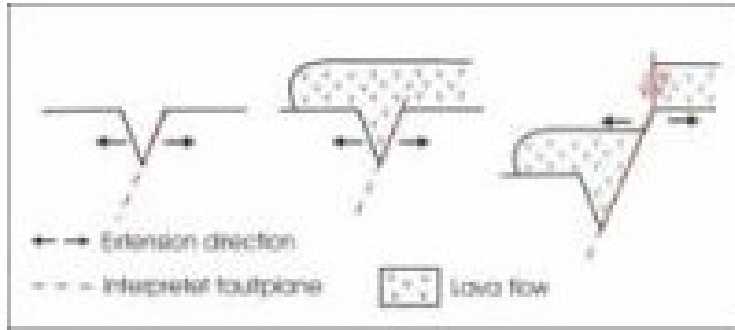


Figure 2.26 Sketch showing the first model for the development of the above fault. After the development of a fissure, a basalt flow erupts and covers it. Later the fault gets a horizontal displacement. From left to right.

Another fault model is also proposed for high scarps of greater than 20m, faults without any opening or horizontal displacement (figure 2.27). In these faults, the formations of snake shaped extension fractures are interpreted as the first stage. Next transformation of these fractures into deep, bigger fissures and open faults with small vertical displacements is interpreted as the second stage. The last stage is the development of a mature fault having a vertical displacement of up to 25m. It is proposed that, the original fissures and fractures are filled with either volcanic material erupted through them or sediments, so that horizontal displacement is not visible any more.



Figure 2.27 A fault with high vertical displacement but devoid of an opening.

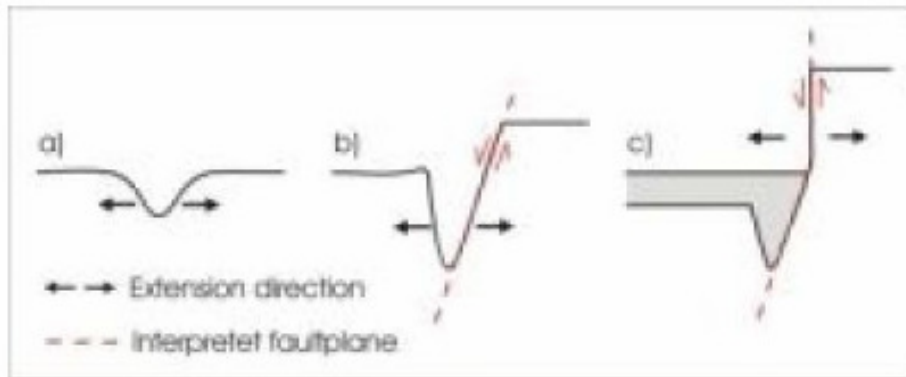


Figure 2.28 Schematic sketch of second model for the development faults in the area.

2.2.2.4 Fault Kinematics

The kinematics of most of the Ethiopian Rift faults has been determined in suitable sites of measurements which are mostly collected in Plio- Quaternary rocks. Most of these data showed, a roughly E – W direction of extension which is oblique to the Main Ethiopian Rift trend.

In the investigation area, it was difficult to get matching edges from faults. However, some kinematic data were collected in Danisa and Salen areas from matching pairs of cooling fractures on the opposite walls (figure 2.29 and 2.30). The collected field data with opening directions and horizontal displacements are further evaluated using the formula

$$T = \frac{\sum_{i=1}^{n=30} Od * HD}{\sum_{i=1}^{n=30} HD}$$

Where, T is total weighted opening direction

Od is approximate opening direction

HD is horizontal displacement

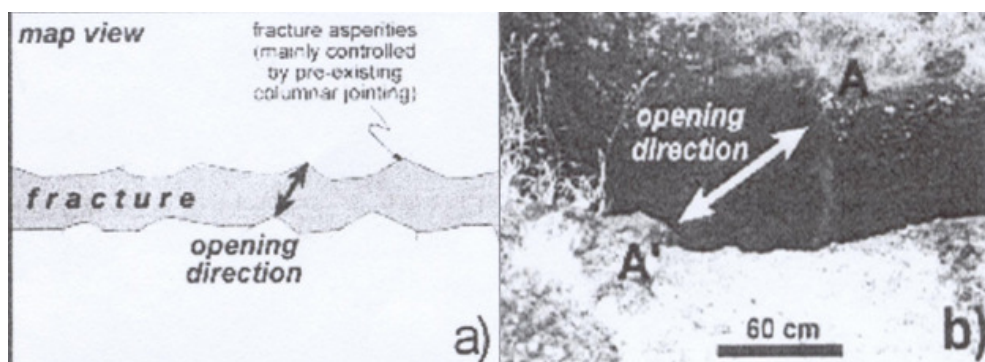


Figure 2.29 Determination of opening direction by matching pairs of cooling fractures on the opposite walls (after (Acocella and Korme, 2002)).

About ten kinematic data collected from Danisa area (Appendix 2a) were further analyzed and gave an average extension direction of 95° . Similarly about 32 kinematic data collected from matching edges of cooling fractures in salen area (Appendix 2b) gave an average direction of 92° .

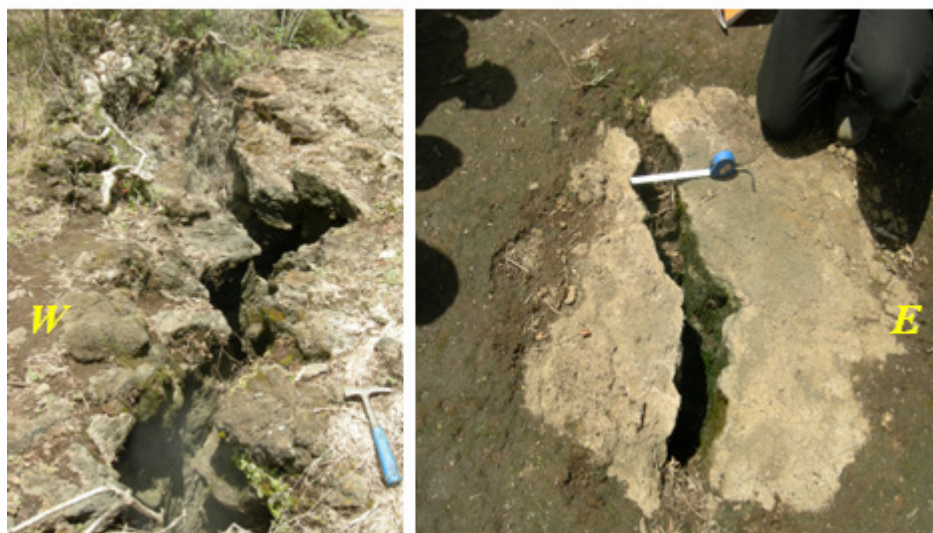


Figure 2.30 Matching edges from cooling fractures, Salen/ Tero area.

Generally based on general fault patterns in the area and structural analysis made on the two site above, the Quaternary evolution of the area is consistent with a nearly E – W direction of extension.

3. FAULTING AND MAGMATISM

The general Quaternary tectonic setting of the main Ethiopian Rift is controlled by the en echelon arrangement of the WFB (Mohr, 1962). These NNE – NE Quaternary rift zones of the WFB form areas of active deformation obliquely cutting the rift floor in MER (Bocaletti et al., 1998; Abebe et al., 2007). Volcanism in the Main Ethiopian Rift is characterized by a bimodal basalt- rhyolite association (Abebe et al., 2007).

Previous studies (Ebinger, C., Casey, M., 2001) on MER showed that, there are many Quaternary magmatic segments arranged in right stepping en echelon fashion among which the Koka magmatic segment represent large portion of the study area. Volcanism in the magmatic segments commenced about 1.6 Ma. Most flows emanated from fissures and small cinder cones (WoldeGabriel et al., 1990; Boccaletti et al., 1999). Quaternary basaltic volcanism in the MER is mainly concentrated along the orientation of faults and fractures of the WFB. These eruptions are controlled by extension fractures with chains of scoria cones developed along the fractures. Likewise in the study area most of the recent basalts and obsidian domes are clearly cut by the WFB fractures and normal faults (figure 3.2). In addition to the interaction of faults/ fractures and basaltic eruptions, the alignment of scoria cones along faults is the other interesting feature. GPS inventory of cones location in the area (figure 3.1) showed that, they are aligned with an approximate strike of SSW-NNE. Moreover, some of these cones are elongated and their maximum basal diameters parallel to the axial faults in the area. Particularly in the southern crater rim of Gedemsa, the faults continue to the south and several cones are connected to them. Fascinatingly, the cones are situated on the foot wall of the normal fault or have their center on the fault but never on the hanging wall.

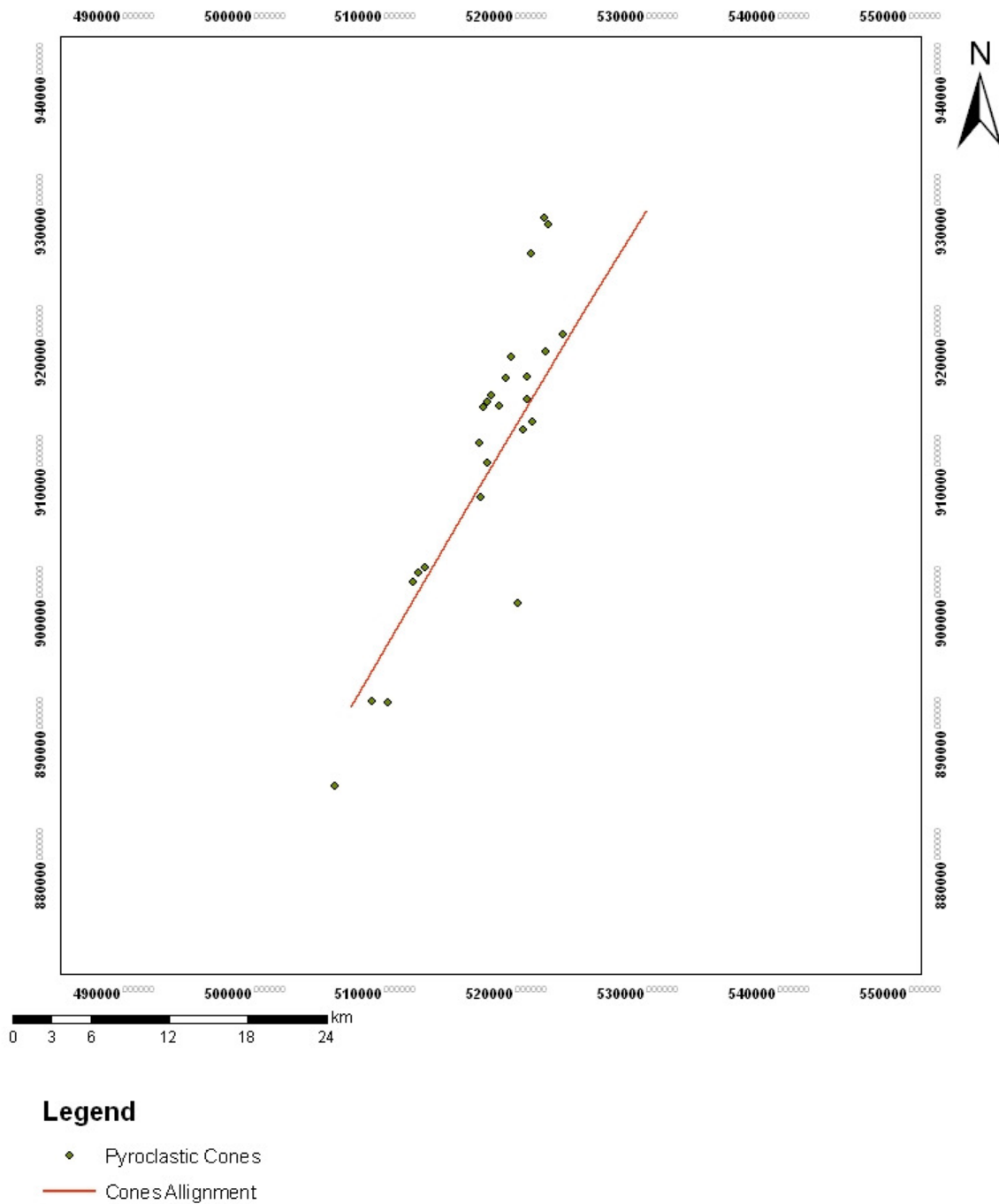


Figure 3.1 Map showing pyroclastic cones with their approximate alignment.

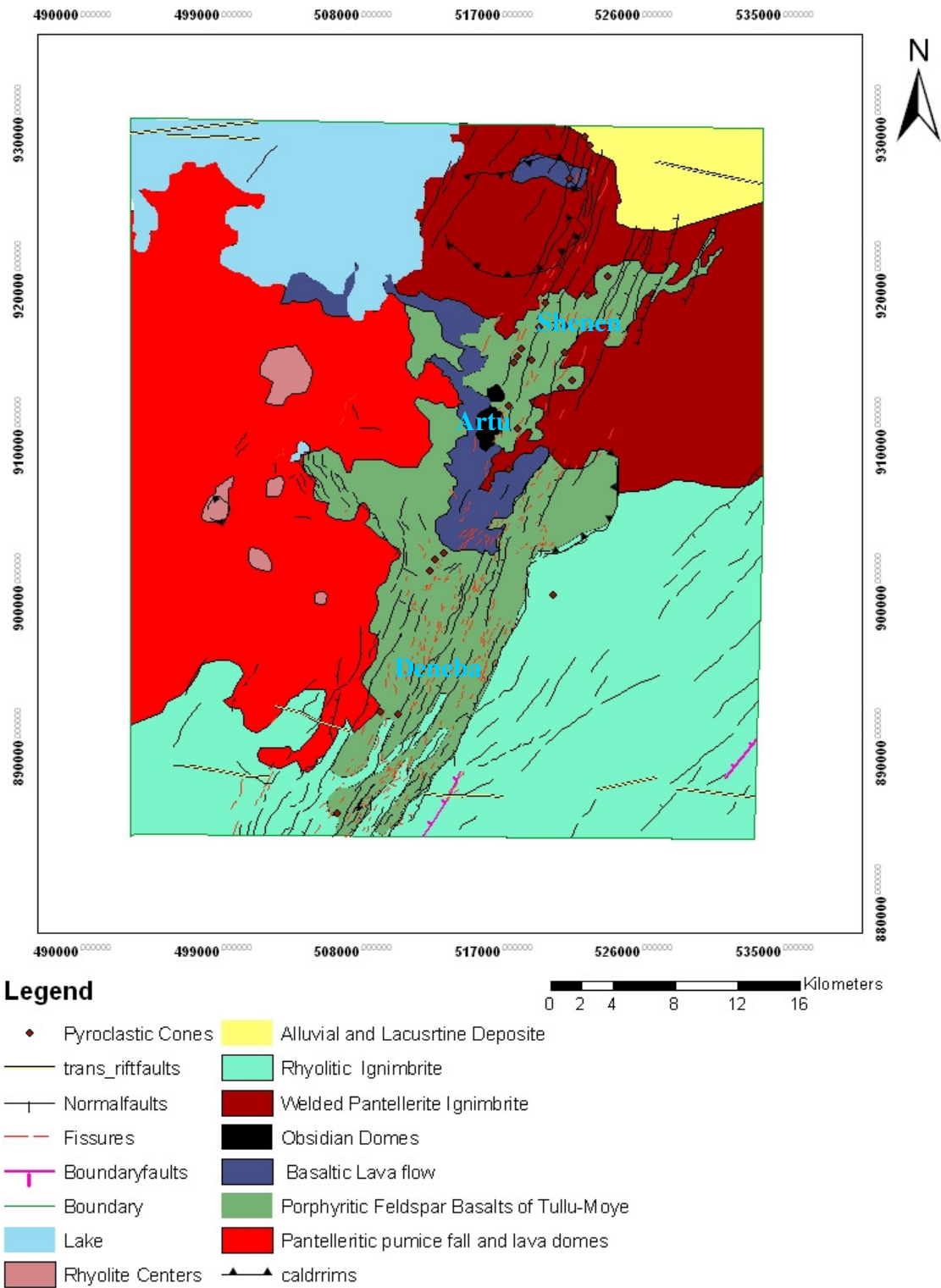


Figure 3.2 Volcano – tectonic map of the area

Large numbers of Plio- Quaternary monogenetic volcanoes in MER are rooted on the fault related open structures such as tail cracks, extensional relay zones and more generally at the intersection of faults (Acocella et al., in press). Fault related open structures are the most appropriate places for outpouring of magma as lava flow and emplacement of monogenetic volcanoes fed by magma chambers situated elsewhere. The major fault related open structures identified in the area are tail cracks, which developed and frequently observed at the termination of NNE striking faults in south of Gedemsa. Tail cracks in MER are the principal locations for emplacement of volcanoes such as scoria cones, lava domes and tuff rings (Korme et al., 1997). Similarly in the study area lava domes and scoria cones are rooted from these NNE striking tail cracks (figure 3.3).

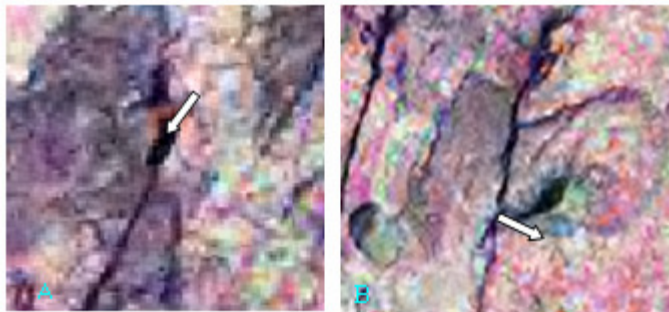


Figure 3.3 Tail cracks from Landsat images arrows showing approximate lava flow directions.

Previously done radiometric ages, as cited below, are collected and adopted for this work. These radiometric ages generally showed some pattern on ageing of magmatism in such away that magmatism is becoming more recent towards the rift floor. For example age dating conducted at the northeast rim of Gedemsa and southern Tulu Moye basalt field showed a relatively recent volcanism. Finally, from the general overview of MER magmatism and this simple age observations, magmatism in Main Ethiopian Rift is becoming more localized.

Table 3.1 Radiometric dates of rocks from Asella and Gedemsa areas.

No.	Rock Type	Location	Age- K/Ar (Ma)
1	Dike cutting ignimbrite	Asella area	1.77±0.44
2	Ignimbrite along escarpment	Asella	1.80±0.09
3	Pantelleritic ignimbrite	Asella	1.49±0.07
4	Pantellerite ignimbrite	ESE of Gedemsa	1.41±0.07
5	Mugearite lava	West base of Chilalo	1.31±0.13
6	Ignimbrite (glassy fiamme)	Bottom of bawa crater	0.526±0.131
7	Pantellerite Pre caldera lava	SE rim of Gedemsa	0.082±0.021
8	Fiamme of ignimbrite	South of Tullumoye basalt field	0.115±0.016
9	Ignimbrite	Kullumsa cemetery	0.5 (possible age)

Sources: Bigazzai (1993); Zanettin et al., 1980 ; Kunz et al., 1975 ; WoldeGabriel et al., 1990 ; Barebieri et al., 1974.

Generally the interaction between faulting and magmatism in the study area is summarized as follows:

3.1 Cone – Fault interaction

These interactions are mostly found in the northern part of the investigated area (like Daluta, Lugo and Shenan). In these areas, almost all pyroclastic cones have an obvious connection to faults. They are always situated on the foot wall next to the fault. In many cases the fault doesn't have a sharp escarpment next to pyroclastic cone. Mostly faults terminate at the cone and again appear at the other side of it due to a change in behavior of geologic materials as discussed in fault morphology part. The pyroclastic cones are always older than the faults they connect them. There is no clear connection between obsidian cone and faults. Rather, they are cut by extension fractures through which they erupt to the surface for example in Artu area.

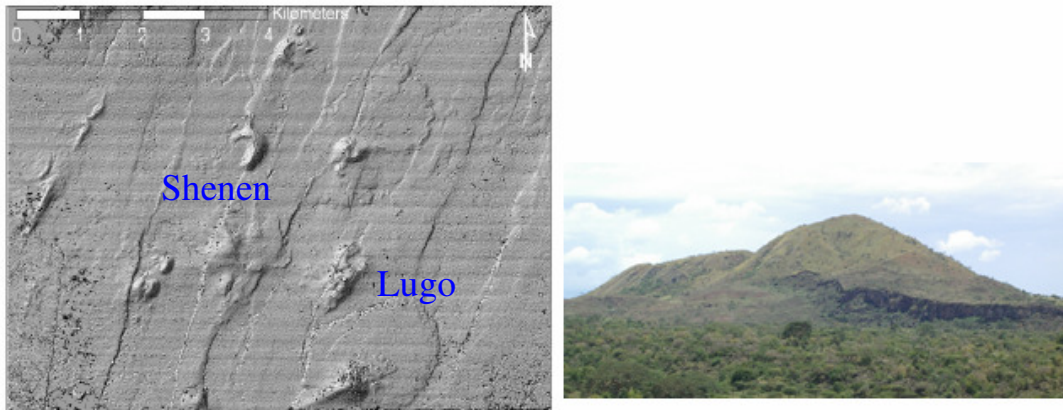


Figure 3.4 DEM of south of Gedemsa. (After Martina, 2005)

3.2 Cone – Basaltic lava flow interaction.

Cone – lava flow interactions are also observed at the northern edge of the study area. In Shenen and Lugo areas, most pyroclastic cones are situated at relatively elevated position whereas, the associated lava flows are situated at the base of cones overlying the pyroclastics. Lava flows seem to be originating from these cones and flow towards the lower elevation areas. From this cone – lava flow interactions, the possible model that can be proposed is as follows: First, there was an eruption with pyroclastic materials which further generated these pyroclastic cones. Later a second eruption with lava flow come and even overprints the original shapes of the cones (figure 3.5).



Figure 3.5 Lava flow overprinting the pyroclastic cone.

3.3 Fault – Basaltic lava flow interactions.

Fault and basaltic flow interactions are observed at the southern and central parts whereas lava flows are mostly prominent on the northern part of the study area. In a general sense, recent basalts (vesicular and porphyritic) in Deneba, Danisa and Artu areas are situated on grabens bounded by larger and relatively old faults. Particularly, fault and basaltic flow interaction in Deneba area is more evident in such a way that, basaltic flows are usually aligned with the faults and fractures through which they outpoured attaining monocline hanging wall and relatively flat foot wall morphology.



Figure 3.6 Basaltic flows outpoured following Quaternary faults and fractures.

However, in the northern part of the study area, there is no such a clear field evidence for flows which have their origin directly on the fault. As discussed in the lava – cone interactions section above, recently outpoured lava flows covered large portions of Shenene. Change of direction (strike) of faults is clearly observed due to these lava flow outpourings. Otherwise, there is no clear relation between lava flows and normal faults in the area, even the extension fractures are younger than these lava flows.

In general, this study proposes the following model of tectonic development in the northern and southern parts of the study area.

In the central and southern parts, welded ignimbrites are considered as the oldest volcanic product, while faults, basaltic flows and obsidian cones are considered as the younger indications for extensional tectonics.

However, in the northern part of the investigated area, pyroclastic cones are relatively old volcanic product. The younger indications for extensional tectonics are faults, lava flows and obsidian domes, which were generated simultaneously.

4. GEOTHERMAL ACTIVITY

Geothermal energy is an important and promising alternative energy resource that has shown continual growth in this century. The most significant geothermal resources of Ethiopia, identified by surface exploration studies in the late sixties, are located in the Ethiopian Rift valley and in the Afar depression, both belonging to the great East African Rift. Geothermal studies in Ethiopia started back in 1969 by the Ethiopian Government in collaboration with the United Nations Development Program (UNDP). A regional reconnaissance work has been conducted in the whole rift including geology, geochemistry, hydrogeology and remote sensing (UNDP, 1973). This work led to the selection of promising areas among which Tulu Moye is one of the potential areas. The utilization of geothermal resources was only restricted for the use of resort and therapeutic purposes until the end of the year 1998.

Physiographically, thermal sites as well as the entire area are characterized by both mountainous and rough topography. The drainage of the area is generally considered as poor since there are no perennial streams. The central part of the investigated area is strongly affected by thermal activities. The main thermal manifestations are weak fumaroles, active steaming grounds and altered grounds. The manifestations extend from east of Tulu Moye to the south of Berecha volcanic complex. There is a wide area of altered ground in the central part near Salen and Danisa areas. The pyroclastic deposits are highly altered and changed to soft clay-like materials having various colors including whitish, brownish, reddish, and grey.



Figure 4.1 Highly altered pyroclastic material, Salen area

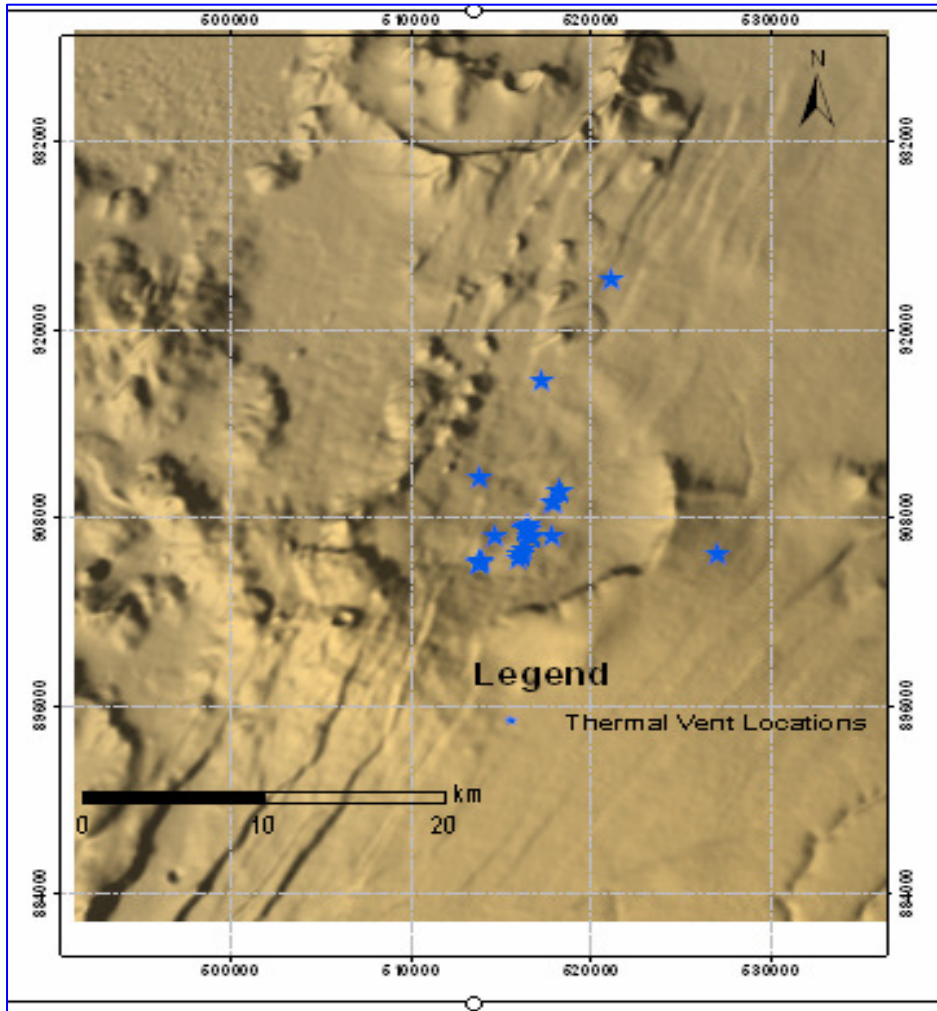


Figure 4.2 Map with distribution of Thermal Vents.

Some of the accessed and surveyed thermal sites in the area include: Hammudie, Tero and Salen/ Danisa. These areas are generally characterized by having relatively large areas of altered zone like south of Hammudie, central Artu and Salen areas. They are also highly affected by hydrothermal activities and there are extensive areas of thermal manifestations characterized by surfacial alterations that usually include reddish clay materials. There are fumaroles and warm grounds. The fumaroles give a

special hissing sounds indicating that they are really powerful vents. The local people use these fumaroles for balneological purposes.



Figure 4.3 Fumaroles used for balneological purpose.

These thermal sites are highly influenced by dense and intense faulting and fracturing. The fractures/ fissures of relatively small to large size are densely populated through which the fumaroles are raised up ward to the surface.

It is generally true that, stratigraphy and volcanism influence the development of geothermal resources. However, structures and tectonics also strongly affect these thermal systems. The aim of this study is therefore, to give some general idea about the effect of structures on thermal sites based on fault/fracture geometry and thermal vent location.

The hydrothermal activities of the mapped area are mainly concentrated close to the silicic centers and generally follow the normal NNE- SSW running block faults and fractures. Close observation has been made in Artu, Danisa and Tero areas. These areas are located at the center of the study area. After some tens of kilometers west of Iteya, there are relatively large NNE striking faults with down throws to wards the west and symmetrically other faults are running in the same direction further far to the west leaving a faulted graben in between. All the above selected thermal sites as well as the inventoried thermal vents (Appendix 3) are contained within this graben.

This graben area is topographically characterized by peaks covered with obsidians and porphyritic basalts of Tulu Moye and flat areas occupied by sediments and recent vesicular basalts. Small to large sized fissures and fractures are typical in these areas, cutting obsidians and basalts at places. In Salen area for example, obsidian domes are also cut by wide fractures through which these active fumaroles are rising up ward as shown in figure 5.4. All fractures in the area have almost the same orientation of about 5° to 10°N striking and openings ranging from 10cm to 3m.



Figure 4.4 Active fumaroles on relatively elevated obsidian dome, Salen area.

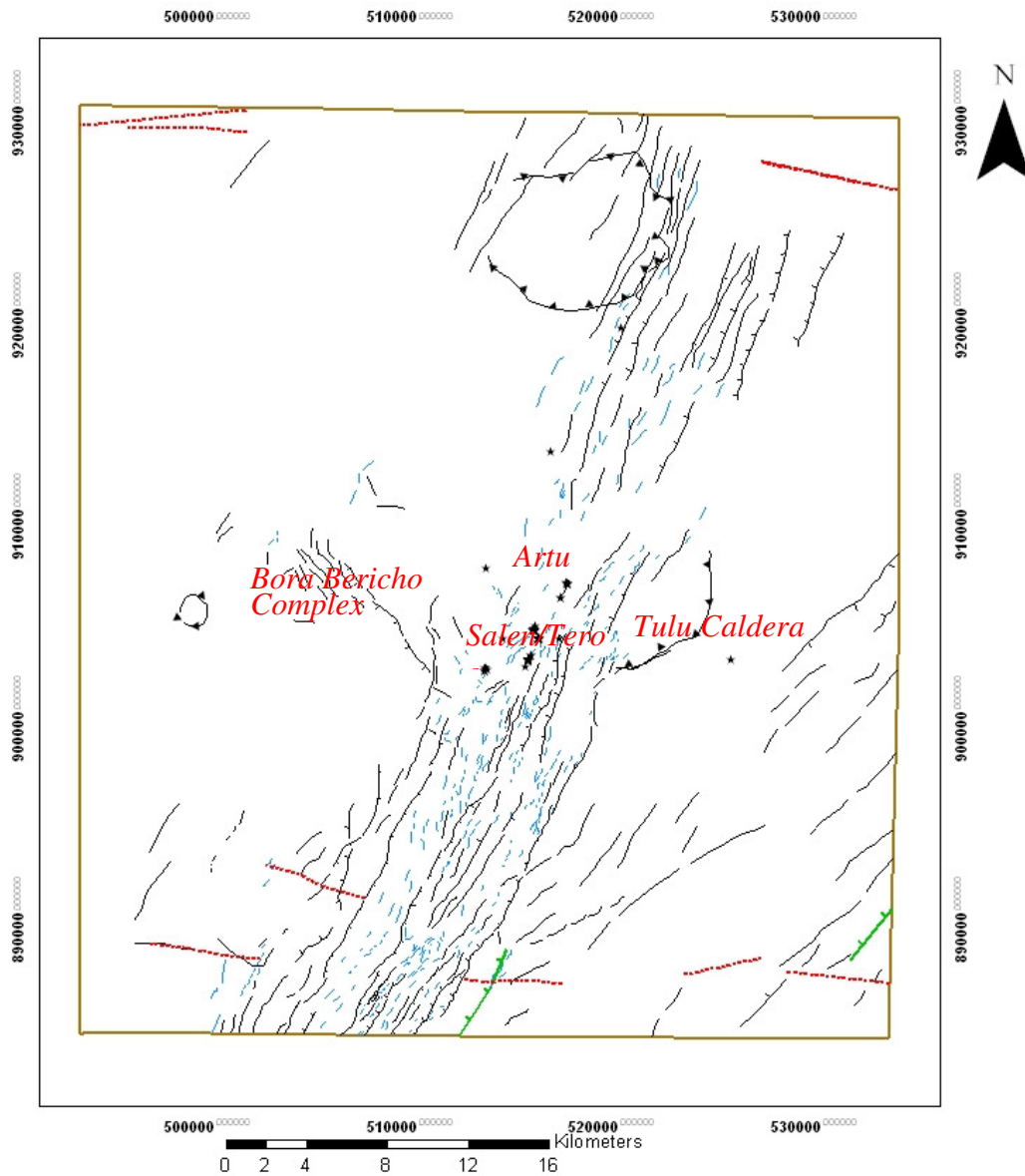


Figure 4.5 Fractures of Various size through which fumaroles raises up. Artu area.

As shown in figure 4.6 below, the graben where most of the inventoried fumaroles are located seems to be affected by four sets of structures namely: the NNE-SSW trending extensional fractures/fissures running from south to north of the study area, the NE-SW trending normal faults, the NW-SE trending cross-rift normal faults near Bora Brioche mountain and Tulu

caldera to the eastern side. So the interaction of all these structures in the area created favorable conditions for the existence of thermal sites by increasing permeable pathways for the infiltration of meteoric water in the ground. According to Tamiru Alemayehu and A. Vernier (1997), heat source for thermal activities in Main Ethiopian Rift is located at relatively shallow depth (for example about 400m in Boku caldera). Likewise, due to intensive faulting and fracturing in the area the crust get thinned and shallow magma chambers may be located at few kilometers depth.

The necessary conditions for the existence of geothermal system are heat source, reservoir, recharge and cap rock. However in continental rift zones like Ethiopian Rifts, many areas have big heat source but lack groundwater recharge since most of the Ethiopian Rivers drain away from the rift margin. Like wise these thermal sites in the area lack groundwater recharge due to rough topography. Eventhough, there may be some recharge to the graben floors. So these dense fractures and normal faults as well as Tulu Caldera in the area play a significant role as a conduit or pathways for the infiltration of meteoric water in to the ground. This infiltrated meteoric water circulates through these fractures, gets heated by shallow seated magmas and finally comes up ward through this high permeability fracture pathways.



Legend

- ▲▲ Caldera rims
- Trans_rift faults
- | Normal faults
- Fissures and fractures
- | Boundary faults
- Boundary
- * Thermal Vent Locations

Figure 4.6 Map showing the interaction of structures and vent locations alignment.

4.1 Application of remote sensing in geological investigation

Geological mapping involves recording geological information on to a map. The geological information includes the distribution, nature and age relationships of the rock units and the occurrence of structural features, mineral deposits and geothermal resources. Since conventional geological mapping involves men working in the field and logistics, it is time, cost and effort-consuming work. In contrast, remote sensing images that cover large area with in short time and low cost are usually used for geological explorations before conducting field works. Remote sensing sensors can detect different reflectance beyond that the human eye can detect that is limited to the visible portion of electromagnetic spectrum

Estimation of Land Surface Temperature (LST) from remotely sensed data is nowadays usual. LST is a key parameter in the physics of land surface processes because it is involved in the energy balance as well as in the evapotranspiration and desertification processes (Peres and DaCamara, 2004). The extensive requirement of land surface temperature (LST) for environmental studies and management activities of the Earth's resources has made the remote sensing of LST an important academic topic during the last two decades (Sobrino, et al., 2004). One of the most important parameters in all surfaces-atmosphere interactions and energy fluxes between the ground and the atmosphere is land surface temperature (Sobrino, et al., 2003).

The Landsat ETM+ with 60m spatial resolution of thermal infrared band enables users to define the more detailed surface temperature. Different algorithms or procedures were carried out to derive the surface temperature, generate the temperature color map and analyze the data. Among these conversion of Digital number (DN) to spectral radiance and conversion of spectral radiance to temperature are the most commonly used equations (USGS, 2001). Atmospheric or topographic correction is also another process

involved for the elimination of atmospheric and illumination effects to retrieve physical parameters of the Earth's surface example surface reflectance, emissivity, and temperature. Likewise land surface temperature map of the central sector of MER is produced by Khalid Adem. So that the land surface temperature anomaly of the study area is taken and adopted for this work just to show the relationship between thermal sites, land surface temperature and lineaments in the area.

4.2 Interpretation of Land Surface Temperature (LST).

Figure 4.7 shows the surface temperature distribution of the area. From this map the northeastern and southern parts of the mapped area characterized by having larger temperature anomaly range. Whereas, Tulu Moye and Iteya areas fall in medium to high range of temperature. But at large scale, it is observed that most of the inventoried fumaroles at central Tulu Moye fall on the high temperature range sites.

From previous sections, it is shown that most of the lineaments (normal faults and fractures/fissures) in the area are densely concentrated relatively on the eastern part of the mapped area having an approximate orientation of NNE. As shown in figure 4.8, the brighter or high temperature anomaly areas clearly delineate the fault traces and all the inventoried thermal fumaroles fall within this relatively high temperature ranges.

Generally this section shows a clear relation of surface temperature anomaly, thermal vent distribution and structures indicating that area is characterized by active volcano-tectonic history.

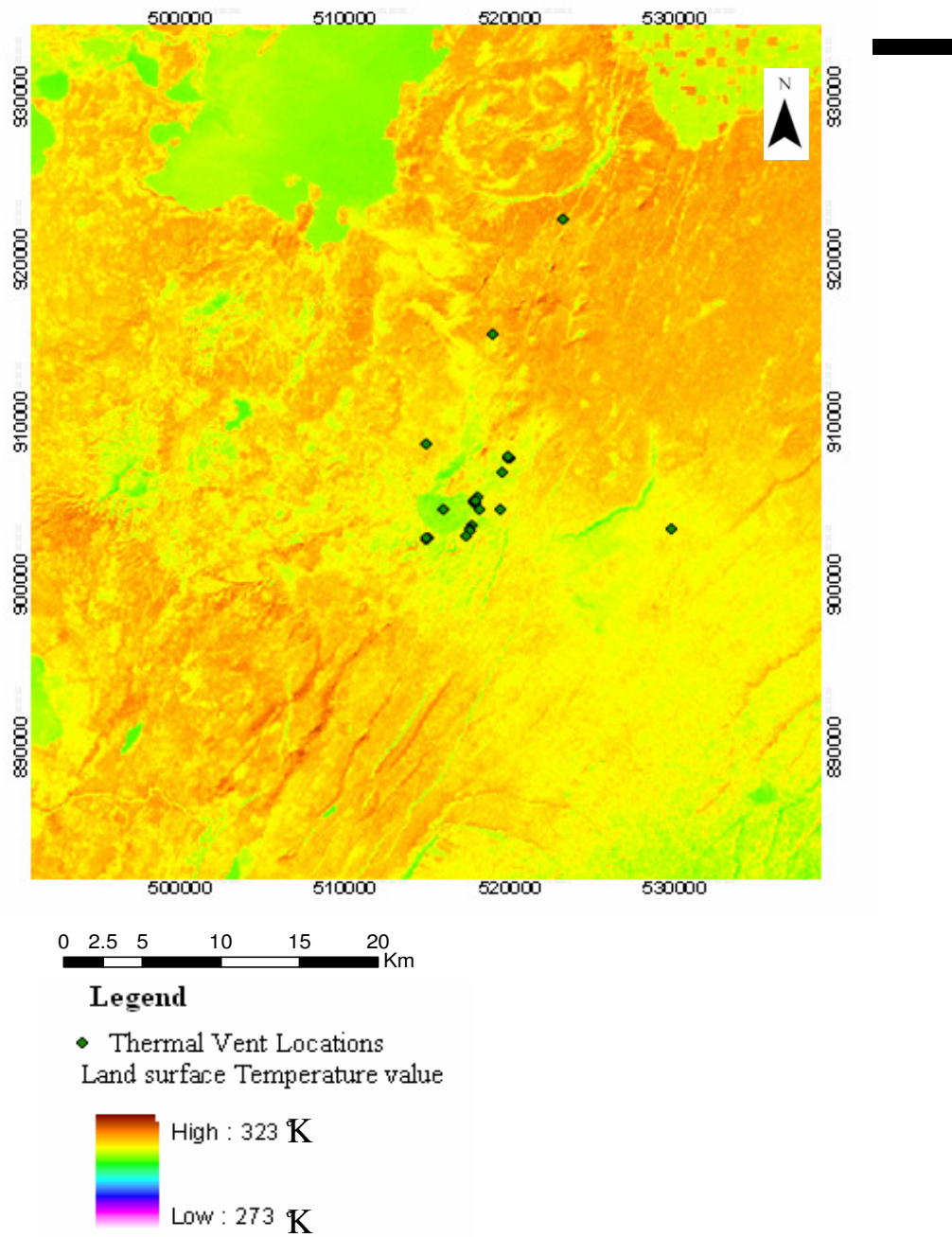


Figure 4.7 Land Surface Temperature map of the area with Thermal Vents Distribution.

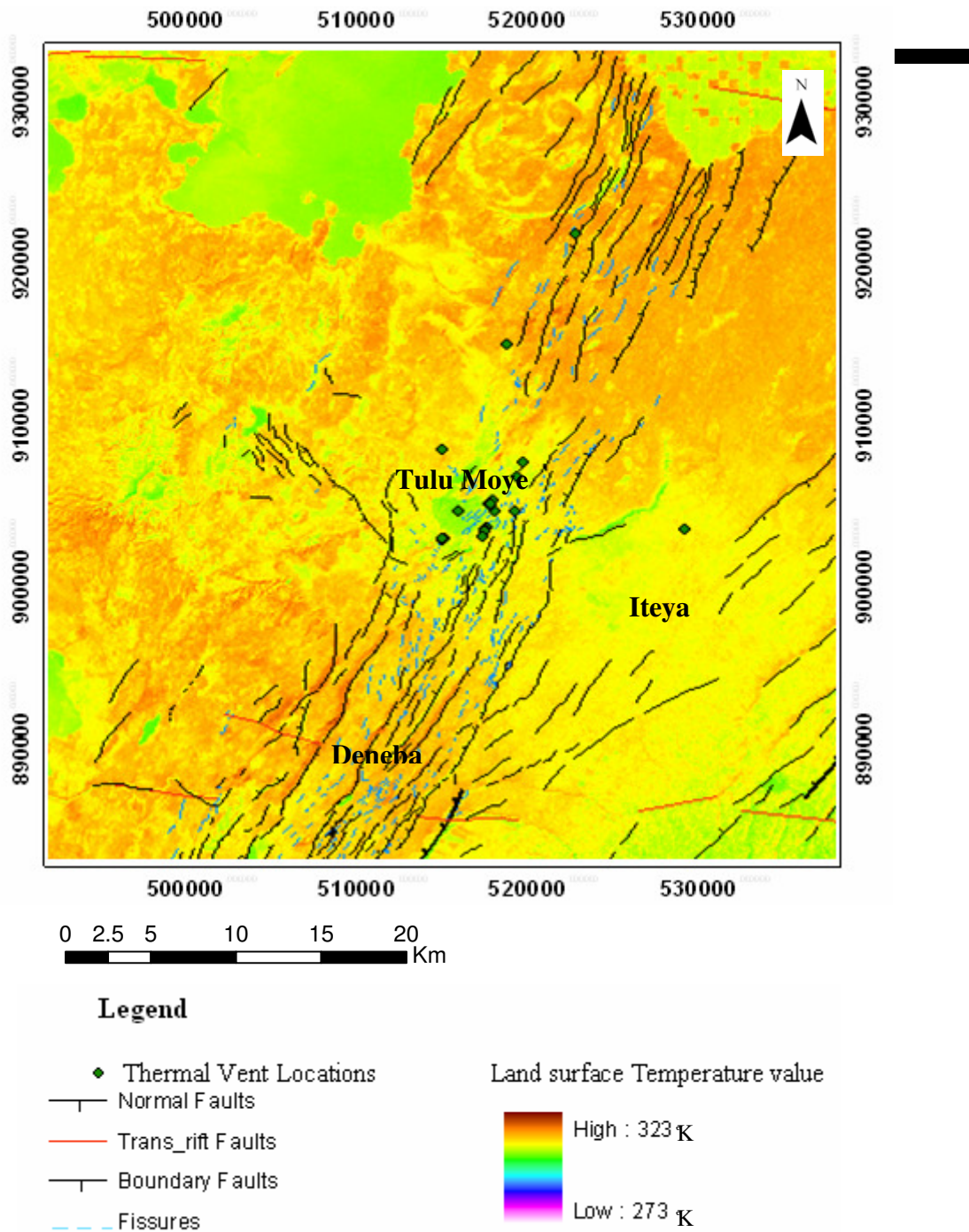


Figure 4.8 Overlay map of Land Surface Temperature, Thermal vents and Lineaments.

5. CONCLUSION AND RECOMMENDATIONS

6.1 Conclusions

Based on the integrated geological, structural and thermal investigations in Tulu-Moye and its surrounding areas, this study led to the following conclusions. It is important to note that the nature and content of conclusions are limited by and to the extent of data available.

Volcano- tectonic map has been produced in order to investigate the Quaternary tectonic and volcanic relationships in the studied area. This map is produced from the inventory of the Quaternary fault patterns and volcanic products, which in turn were made from detailed interpretation stereoscopic pairs of air photographs (1:50,000) and on screen digitization from Landsat imageries of 28.5m resolution. Therefore, the oldest volcanism is at the rift shoulder (Eastern margins) as well as the last period of volcanic activity developed along the Wonji Fault Belt (WFB) in such a way that, volcanism is becoming more recent and young towards the central part of the area or axial zone generally speaking.

From the interpretation of Landsat images and air photos supported by field observations, generally three sets of extensional structures are mapped. These are 1) NW – SE striking rift margin normal faults 2) NW –SE and E – W Striking cross – rift faults and 3) NNE – SSW and N- S trending youngest rift faults.

Morphologically most of the surveyed faults are of non flexural types, having almost flat foot wall and hanging wall tilted away from the fault plane. Generally two types of fault models are proposed in the area and in addition an approximate E – W direction of extension is obtained from collected kinematic data.

Inventory of thermal vents using GPS has been made in the investigated area with close observation on how they are related with structures and volcanic activities. The observation made in place showed that most of the steamings

in the area rose up to the surface through these active and dense fractures/ fissures and also all thermal sites are located on the graben between faults running in NNE – SSW direction. This field observation is also consistent with the map produced from the overlay of structures and thermal vent locations. Generally, densely populated Quaternary fractures/fissures and block normal faulting in the area act as a conduits or pathways for circulation of meteoric water. Therefore, from the abundance of different acidic lavas, recent eruption due to tensional tectonics, dense and intensive faulting/ fracturing, and wide thermal activities, the Tulu Moye geothermal prospect is believed to be the an area with exploitable geothermal resource.

6.2 Recommendations

Due to the rough topography and absence of routes, accessibility to some localities in the area is rather difficult and so most previous studies are done based on techniques of remote sensing and GIS. Nevertheless, since the area is very active in both extensional tectonics and volcanic activities, accessing and close observations are rather advisable since lithologic and structural mapping from satellite imageries has certain drawbacks and uncertainties.

It is true that structures are the basic features controlling the thermal activities in the area, so detailed structural investigation should be carried out, especially on the central part of the area for a better definition of these anomalous zones.

Detailed geology and localized stratigraphy of the area should be made to determine the best permeable reservoir and cap rock, since they are the necessary conditions for the existence and development of geothermal resources.

REFERENCE:

- Abebe, B., Acocella, V., Korme, T., Ayalew, D., 2007. Quaternary faulting and magmatism in the Main Ethiopian Rift. *Journal of African Earth science*, 48, 115-124.
- Abebe, B., Boccaletti, M., Mazzuoli, R., Bonini, M., Tortorici, L., Trua, T., 1998. Geological map of the Lake Ziway – Asella region (Main Ethiopian Rift). Scale 1:50,000.
- Abebe, T. 2000. Geological limitations of a geothermal system in a continental rift zone: example the Ethiopian Rift Valley. *World Geothermal Congress. 2025 - 2030*
- Abebe, T., Mazzarini, F., Innocenti, F., Manetti, P., 1998. The Yerer – Tullu Wellel volcanotectonic lineament: a transtensional structure in central Ethiopia and the associated magmatic activity. *Journal of African Earth Science*. 26, 135 – 150.
- Acocella, V., Gudmundsson, A., Funiciello, R., 2000. Interaction and linkage of extensional fractures: examples from rift zone of Iceland.
- Acocella, V., Korme, T., 2002. Holocene extension direction in the axial zone of the Main Ethiopian Rift. *Terra Nova*, in press.
- Acocella, V., Korme, T., Salvini, F., 2002. Mechanism of fault formation along the axial zone of Main Ethiopian Rift. *Journal of Structural Geology*. 191-197.
- Acocella, V., Korme, T., Salvini, F., 2003. Formation of normal faults along the axial zone of the Main Ethiopian Rift. *Journal of structural geology*, 25, 503-513.
- Alemayehu, T., Vernier, A., 1997. Conceptual model for Boku hydrothermal area. Main Ethiopian Rift. *SINET. Ethiopian Journal of Science*, 20, 283-291.
- Alula, D., Boccaletti, M., Getaneh, A., Mazzouli, R., Tortorici, L., Trua, T., 1990. Geological map of Nizreth – Dera region (Main Ethiopian Rift). Scale 1:50,000.

- Angier, J., Bergerat, F., Dauteuil, O., Villemin, T., 1997. Effective tension-shear relationship in extensional fissure swarms, axial rift zone of northeast Iceland. *Journal of structural geology*, 19, 673-685.
- Barberi, F., Boatti, E., Marinelli, G., Vareti, J., 1974. Transverse tectonics during the split of a continent: data from Afar rift. *Tectonophysics*, 23, 17-29.
- Bigazzi, B., Bonadonna, F., Di Paola, G., Giuliani, A., 1993. K-Ar and fission tracks ages of the last volcano-tectonic phases in the Ethiopian Rift Valley (Tulu Moye area). *Geology and mineral resources of Somalia and Surrounding Regions*. 113, 311-322.
- Boccaletti, M., Bonini, M., Mazzuali, R., Abebe, B., Piccardi, L., and Tortorici, L., 1998. Quaternary oblique extensional tectonics in the Ethiopian Rift (Horn of Africa). *Tectonophysics*, 287, 97-116.
- Boccaletti, M., Mazzuoli, R., Bonini, M., Trua, T., and Abebe, B., 1999. Plio-Quaternary volcano tectonic activity in the northern sector of the Main Ethiopian Rift: relationship with oblique rifting. *Journal of African Earth Science*, 29, 679-698.
- Bonatti, E., 1985. Punctiform initiation of seafloor spreading in the Red Sea during transition from a continental to an oceanic rift. *Nature*, 316, 33-37.
- Bosworth, W., 1985. Geometry of propagating continental rifts. *Nature*, 316, 625-627.
- Buck, W., 1991. Modes of continental lithospheric extension. *Journal of geophysical research*, 96, 20161-20178.
- Chernet, T., Hart, W., Aronson, J.L. and Walter, R.C., 1998. New age constraints on the timing of volcanism and tectonism in the northern Ethiopian Rift- southern Afar transition zone (Ethiopia). *Journal of Volcanology, Geothermal Resource*. 80, 267-280.
- Chernet, T., Hart, W. K., 1999. Petrology and geochemistry of volcanism in the northern Ethiopian Rift- southern Afar transition region. *Acta Volcanology*. 11, 21-42.

- Chorowicz, J., Collet, B., Bonavia, F., and Tesfaye Korme (1994). Northwest to north-northwest extension direction in the Ethiopian Rift deduced from the orientation of extension structures and fault slip analysis. *Geological Society of American Bulletin*. 105:1560 – 1570.
- Davidson, A. and Rex, D.C., 1980. Age of volcanism and rifting in southwestern Ethiopia. *Nature*, 283, 657-658.
- Di Pola, G.M. 1970. Geological and Geothermal report on the central part of the Ethiopian Rift Valley. Ministry of Mines Addis Ababa Ethiopia. Unpublished. 1 - 46.
- Di Pola, G.M. 1971. Geology of Corbetti caldera area, Main Ethiopian Rift, Department of Mineralogy and Petrography, University of Pisa, Italy.
- Di Pola, G., 1972. The Ethiopian Rift Valley (between 7°00' and 8°40' Lat. North). *Bulletin of Volcanology*, 35, 497-506.
- Di Pola, G.M. 1977. Geological map of Tulu Moye volcanic area. Scale (1:75,000).
- Ebinger, C., Crow, M., Rosendahl, B., Livingstone, D., Lefoumier, J., 1984. Structural evolution of Lake Malawi. *Africa nature*, 308, 627-629.
- Ebinger, C., Rosendahl, B., Reynolds, D., 1987. Tectonic model of Malawi rift, Africa. *Tectonophysics*, 141, 215-235.
- Ebinger, C., 1989. Geometric and kinematic development of border faults and accommodation zones. *Tectonics*, 8, 117-133.
- Ebinger, C and Hayward, N., 1996. Soft plates and hot spots: Africa *journal of geophysics*, 21, 859-876.
- Ebinger, C., Casey, M., 2001. Continental breakup in magmatic provinces: An Ethiopian Example. *Geological Society of America*. 29, 527-530
- Ebinger, C. J., Yemane, T., WoldeGabriel, G., Aronson, J.L., Walter, R.C. 1993. Late Eocene – Recent volcanism and faulting in the southern Main Ethiopian Rift. *Journal of geological society*. London, 150, 99 – 108.

- Electroconsult, ELC, 1986. Geothermal exploration project- Ethiopian lakes district, exploration of Langano-Aluto geothermal resources, feasibility report. Pp 150.
- EIGS (Ethiopian Institute of Geological Surveys. Ministry of Mines and Energy), 1987. Geological map of Nazreth sheet, scale 1:250,000.
- ELC and EIGS, 1987. Geothermal reconnaissance study of selected sites of the Ethiopian rift.
- Forslund, T., Gudmundson, A., 1991. Crustal spreading due to dikes and faults in southwest Iceland. *Journal of structural geology*, 13, 443-457.
- Gibson, I., 1969. The structure and volcanic geology of an axial portion of the Main Ethiopian Rift. *Tectonophysics*. 8, 561-565.
- Gianelli, G., Teklemariam, M., 1993. Water – rock interaction processes in the Aluto- Langano geothermal field. *Journal of Volcanology and Geothermal Resource*. 56, 429 – 445.
- Gudmundsson, A., 1987a. Geometry, formation and development of tectonic fractures on the Reykjanes peninsula, southwest Iceland. *Tectonophysics*, 139, 295-308.
- Gudmundsson, A., 1992. Formation and growth of normal faults at the divergent plate boundary in Iceland. *Terra Nova* 4, 464 – 471.
- Hardbeck and Hauksson, 1999. Fracturing and hydrothermal alterations in normal fault zones. *Pure and Applied geophysics* 142, 609-644.
- Hart, W., WoldeGabriel, G., Walter, R., Mertzman, S., 1989. basaltic volcanism in Ethiopia. Constraints on continental rifting and mantle interactions. *Journal of geophysics*, 94, 7731-7748.
- Kazmin, V., Byankov, A., 2000. Magmatism and crustal accretion in continental rifts. *Journal of African Earth Sciences*, 30, 555-568.
- Kazmin, V., 1972. Geological map of Ethiopia. Scale (1:2000, 000). Geological survey of Ethiopia, Ministry of Mines, Addiss Ababa.
- Kazmin, V., Seife, M., Nicoletti, M., Petrucciani, C. 1980. Evolution of the northern part of the Ethiopian Rift, in geodynamic evolution of the Afro-Arabian Rift System. 275-292.

- Korme, T., Acocella, V., 2002. Holocene extension direction along the Main Ethiopian Rift, East Africa. *Terra Nova*, 14, 191-197.
- Korme, T., Acocella, V., and Abebe, B. 2003. The role of pre-existing structures in the origin, propagation and architecture of faults in Main Ethiopian Rift.
- Korme, T., Chorowicz, J., Collet, B., and Bonavia, F.F., 1997. Volcanic vents rooted on extension fractures and their geodynamic implications in the Ethiopian Rift. *J. Volcanol. Geotherm. Res.*, 79, 205-222.
- Kunz, K., Kreuzer, H., Muller, P., 1975. Potassium-Argon age determinations of the Trap basalt of southeastern part of Afar rift. *Afar depression of Ethiopia. Schweizerart, Stuttgart*, Pp. 370-374.
- Kurz, T. 2004. Localization of the deformation in the Main Ethiopian Rift a remote sensing study. Unpublished master's thesis, TU Bergakademie Freiberg. Pp. 30.
- Lavitte, D., Columba, J., Mohr, P., 1974. Reconnaissance geology of the Amaro Horst, southern Ethiopian Rift. *Geological society American Bulletin*, 85, 417-422.
- Martina, B. 2005. Structural studies in the Main Ethiopian Rift, south of Gedemsa. Unpublished study.
- Martinez, F., Cochran, J., 1988. Structural and tectonics of the northern Red Sea: catching a continental margin between rifting and drifting. *Tectonophysics*, 150, 1-32.
- McKenzie, D., Davides, D., Molnar, P., 1970. Plate tectonics of Red Sea and East Africa. *Nature*, 226, 243-248.
- Merla, G., Abbate, E., Azzaroli, A., Bruni, P., Canuti, P., Fazzuali, M., Sagri, M., Tacconi, P., 1979. A geological map of Ethiopia and Somalia, and comment. CNR, Firenze.
- Meseret, T., Kibret, B., Yiheyis, A., Zewde, G. 2000. Geothermal development in Ethiopia. Unpublished.

- Meyer, W., Pilger, A., Rosler, A., Slets, J., 1975. Tectonic evolution of the northern part of the Main Ethiopian Rift in southern Ethiopia. Pp. 352-362.
- Mohr, P., 1962. The Ethiopian Rift System. *Nature*, 5, 33-62.
- Mohr, P., 1967. Major volcano-tectonic lineament in the Ethiopian Rift System. *Nature*, 213, 664-665.
- Mohr, P., 1968. Transcurrent faulting in the Ethiopian Rift System. *Nature* 218, 938 – 941.
- Mohr, P., 1970. *The Geology of Ethiopia*. Addis Ababa University Press. Addis Ababa. Pp 1-268
- Mohr, P., 1983. Ethiopian flood basalt province. *Nature* 303, 577 – 584.
- Mohr, P., 1987. Pattern of faulting in the Ethiopian Rift Valley. *Tectonophysics* 143, 169 -179.
- Mohr, P., Mitchell, J.G., Reynolds, R.G.H., 1980. Quaternary volcanism and faulting at O'A caldera, central Ethiopian Rift. *Bulletin of Volcanology*. 43, 173 – 189.
- Needham, H., Choukroune, P., Cheminee, J., Le Pichon, X., Francheteau, J., Tapponier, P., 1976. The accretion plate boundary: Ardoukoba rift (northwest Africa) and the oceanic rift valley. *Earth and planetary science Letters*, 28, 439-453.
- Nelson, R., Patton, T., Morley, C., 1992. Rift-segment interaction and its relation to hydrocarbon exploration in continental rift systems. *American association petroleum geology bulletin*, 76, 1153-1169.
- Peres, F., and DaCamara, C., 2004. Land surface temperature and emissivity estimation based on the two temperature method. *Remote sensing of Environment* 91, 377-389.
- Pollard, D., Delaney, P., Duffield, W., Endo, E., Okamura, T., 1983. Surface deformation in volcanic rift zones. *Tectonophysics*, 94, 541-584.
- Sobrino, J., Jimenez, J., El-Kharazz, J., Gomez, M., Romaguera, M., and Soria, G., 2004. Single channel and two channel methods for land

- surface temperature retrieval. *International Journal of Remote sensing* 25, 215-230.
- Tamsett, D., 1986. Median valley tectonics: air photographs of the Ghouber-Asal rift, Afar. *Tectonophysics*, 131, 75-87.
- Tesfaye, K., 1992. Lithologic and structural mapping of northeast Lake Ziway area, Ethiopian Rift, using Landsat Digital data. Msc. Thesis. Pp. 156.
- Tesfaye, K., 1999. Lithologic and structural mapping of the north east Lake Ziway area, Ethiopian Rift with the help of Landsat TM data. *SINET, Ethiopian Journal of Science*, 22, 151 – 174.
- UNDP, 1973. Geology, geochemistry and hydrogeology of hot springs of the East African Rift System within Ethiopia. New York.
- USGS, Landsat 7 science data users Hand book. Pp. 300.
- WoldeGabriel, G., Aronson, J., and Walter, R., 1990. Geology, geochronology and rift basin development in the central sector of the Main Ethiopian Rift. *Geological society of American Bulletin*, 102. 439 – 458.
- Zanettin, B., Justin, B., Nicoletti, M., Petrucciani, C., 1978. The evolution of the Chenchu escarpment and the Ganuji graben (Lake Abaya) in the southern Ethiopian Rift. *Geological Bulletin*, 8, 473-490.
- Zanettin, B., Justin-Visentin, E., Nicoletti, M., Piccirillo, E., 1980. Correlation among Ethiopian volcanic formations with special reference to the chronological and stratigraphical problems of the Trap series. *Accad. Naz. Deli lincci*, Rome 47, 231-252.

APPENDICES:

Appendix 1. Field measured fault length and vertical displacement (Throw).

No.	Fault length (m)	Vertical displacement (m)	GPS Location	
			Longitude	Latitude
1	2160	25	508527	887532
2	2000	23	509591	886997
3	1800	20	508458	886707
4	1500	15	509388	887797
5	1300	12	511814	885831
6	1100	10	507451	885729
7	800	8	510802	885324
8	600	6	508850	885841
9	500	4	507782	885223
10	400	2	507744	885604
11	200	0	508590	886444

Appendix 2a: Kinematic measured data from Danisa area.

No.	GPS Location		Opening Direction	D i p	Vertical Displacement	Horizontal Displacement	Total Displacement
	Long.	Lat.					
1	515086	897393	062			204	204
2	515152	897538	034			152	152
3	515083	897387	053			173	173
4	515080	897360	051			130	130
5	515350	897831	081			180	180
6	515060	897440	135			150	150
7	514997	897280	116			115	115

Appendix 2b: Kinematic measured data from Salen/Artu areas.

No.	GPS Location		Opening direction	Dip	Vertical displacement	Horizontal displacement	Total displacement
	Long.	Lat.					
1	516330	904639	092			22	22
2	516331	904636	093			20	20
3	516330	904637	094			13	13
4	516326	904631	102			10	10
5	516330	904640	086			15	15
6	516334	904635	116			22	22
7	516323	904634	127			13	13
8	516377	904646	095			15	15
9	516336	904658	091			32	32
10	516341	904663	100			20	20
11	516337	904673	100			23	23
12	516337	904676	098			17	17
13	516336	904640	091			25	25
14	516335	904644	102			18	18
15	516354	904650	305			15	15
16	516353	907430	230			10	10
17	516351	907400	200			20	20
18	516355	907281	110			13	13
19	516380	907286	180			11	11
20	516356	907420	205			12	12
21	516349	907450	250			14	14
22	516099	907287	190			10	10
23	516096	907281	115			15	15
24	516093	907279	135			10	10
25	516098	907277	148			13	13
26	516095	907284	170			18	18

27	516094	907280	127			12	12
28	516090	907282	119			10	10
29	516079	907367	190			12	12
30	516780	907368	165			10	10
31	516000	907378	109			13	13
32	516052	907834	98			11	11

Appendix 3. GPS Locations of Active Thermal vents

No.	Northing	Easting	Elevation
1	903147	516084	2261
2	902939	515994	2181
3	903140	516085	2259
4	902929	515996	1134
5	902924	515995	2213
6	902939	515976	2218
7	902927	515974	2221
8	902926	515971	2223
9	902911	515969	2226
10	902935	515968	2230
11	902965	515954	2230
12	902972	525971	1147
13	902971	515989	2239
14	902965	515984	2241
15	902967	515989	2242
16	902950	515985	2244
17	902882	515965	2245
18	902623	515847	2107
19	902411	513816	2145
20	902408	513820	2149
21	902408	513819	2155
22	902471	513944	2078
23	902501	513849	2080
24	907501	513847	2084
25	902520	513841	2094
26	903983	516469	2042
27	903986	516470	2044

28	903987	516470	2045
29	903990	516473	2046
30	903995	517471	2047
31	903999	516471	2047
32	903995	516471	2049
33	903992	516500	2050
34	903993	516501	2052
35	903992	516499	2052
36	904006	516484	2057
37	904007	514681	2059
38	904017	516481	2059
39	904015	516484	2059
40	904613	516341	2036
41	904406	516233	2038
42	904405	516237	2041
43	904402	516203	2042
44	904406	516286	2059
45	904412	516283	2057
46	904422	516280	2061
47	904379	516267	2056
48	904382	516264	2056
49	904381	516162	2058
50	904470	516223	2047
51	904409	516232	2042
52	904413	516234	2048
53	904425	516239	2049
54	904429	516237	2050
55	904432	516237	2044
56	904426	516236	2047
57	904480	516253	2051

58	904447	516256	2053
59	904448	516265	2054
60	904451	516265	2054
61	905985	517582	1975
62	905984	517561	1979
63	906702	517898	1938
64	906726	517908	1937
65	906707	517929	1938
66	906709	517930	1938
67	906744	517869	1947
68	906754	517869	1945
69	913263	517077	1940
70	919420	520550	1939

Appendix 4. Radiometric dates of rocks from Asella and Gedemsa areas.

No.	Rock Type	Location	Age- K/Ar (Ma)
1	Dike cutting ignimbrite	Asella area	1.77±0.44
2	Ignimbrite along escarpment	Asella	1.80±0.09
3	Pantelleritic ignimbrite	Asella	1.49±0.07
4	Pantellerite ignimbrite	ESE of Gedemsa	1.41±0.07
5	Mugearite lava	West base of Chilalo	1.31±0.13
6	Ignimbrite (glassy fiamme)	Bottom of bawa crater	0.526±0.131
7	Pantellerite Pre caldera lava	SE rim of Gedemsa	0.082±0.021
8	Fiamme of ignimbrite	South of Tullumoye basalt field	0.115±0.016
9	Ignimbrite	Kulumsa cemetery	0.5 (possible age)

Sources: Bigazzai (1993); Zanettin et al., 1980; Kunz et al., 1975; WoldeGabriel et al., 1990; Barebieri et al., 1974.